

Grossular: A crystal-chemical, calorimetric, and thermodynamic study

EDGAR DACHS,¹ CHARLES A. GEIGER,^{1,*} ARTUR BENISEK,¹ AND KLAUS-DIETER GREVEL^{2,3}

¹Fachbereich Materialforschung and Physik, Abteilung Mineralogie, Universität Salzburg, Hellbrunnerstrasse 34, A-5020 Salzburg, Austria

²Institut für Geowissenschaften, Friedrich-Schiller Universität, Burgweg 11, D-07749 Jena, Germany

³Institut für Geologie, Mineralogie und Geophysik, Ruhr-Universität, D-44780 Bochum, Germany

ABSTRACT

In spite of the amount of research that has been done on grossular, $\text{Ca}_3\text{Al}_2\text{Si}_3\text{O}_{12}$, there is still uncertainty regarding its exact thermodynamic properties. Because of insufficient sample characterization in the various published calorimetric studies, it is difficult to analyze conflicting C_p and S° results. To resolve the discrepancies, a detailed and systematic multi-method investigation was undertaken. Three synthetic grossular samples and four natural grossular-rich garnets were characterized by optical microscopy, electron microprobe analysis, IR, and MAS ^{29}Si and ^{27}Al NMR spectroscopy, and X-ray powder diffraction methods. Two of the natural grossulars, crystallized at relatively low temperatures, are optically anisotropic and two from the higher temperature amphibolite facies are isotropic. The natural garnets have between 94 and 97 mol% grossular with minor fractions of other garnet components, as well as small amounts of OH in solid solution. ^{29}Si and ^{27}Al MAS NMR spectra indicate that synthetic grossular crystallized at high- P and high- T conditions is ordered with respect to Al and Si.

Heat-capacity measurements between 5 and 300 K were made using relaxation calorimetry and between 282 and 764 K using DSC methods. For the three synthetic grossulars, the C_p data yield an average S° value of 260.23 ± 2.10 J/(mol·K). The S° values for the four natural grossular-rich garnets, adjusted to end-member grossular composition, range between 253.0 ± 1.2 and 255.2 ± 1.2 J/(mol·K). The results of this work thus confirm earlier low-temperature adiabatic calorimetric studies that show small, but experimentally significant, differences in S° between natural and synthetic grossular samples. The difference in terms of heat-capacity behavior between synthetic and natural samples is that the latter have lower C_p values at temperatures between 20 and 100 K by up to about 20%. Above 298 K, C_p for grossular is given by

$$C_p \text{ J/(mol}\cdot\text{K)} = 556.18(\pm 12) - 1289.97(\pm 394) \cdot T^{-0.5} - 2.44014(\pm 0.24) \cdot 10^7 \cdot T^{-2} + 3.30386(\pm 0.39) \cdot 10^9 \cdot T^{-3}.$$

Applying mathematical programming, published high- P - T results on the reaction 3anorthite = grossular + 2kyanite + quartz were analyzed thermodynamically. The calculations yield best-fit values of $\Delta_r H^\circ = -6627.0$ kJ/mol and $S^\circ = 258.8$ J/(mol·K) for grossular. It is concluded that $S^\circ \approx 260$ J/(mol·K) is the best value for end-member grossular. Variations in structural state and composition in natural samples, as well as assumptions used in correcting for solid-solution and OH groups, appear to be the most important factors that could account for the smaller S° values of 253–257 J/(mol·K).

Keywords: Garnet, grossular, crystal chemistry, spectroscopy, calorimetry, entropy, heat capacity, thermodynamics

INTRODUCTION

Grossular garnet, ideal end-member composition $\text{Ca}_3\text{Al}_2\text{Si}_3\text{O}_{12}$, and grossular-containing garnet solid solutions are important in various rock types of Earth's crust and upper mantle. Many investigations have been directed at understanding grossular's crystal-chemical and thermodynamic properties. For a number of years, considerable effort has been devoted to investigating phase relations in the $\text{CaO-Al}_2\text{O}_3\text{-SiO}_2\text{-H}_2\text{O}$ (CASH) system and, here, grossular plays a central role. This system can be considered as forming a "cornerstone" for various thermodynamic databases. However, in spite of the large and varied amount of research that has been done on grossular, there is still uncertainty regarding its precise thermodynamic properties and phase relations.

* E-mail: ca.geiger@sbg.ac.at

A major issue concerns the value of grossular's standard third-law entropy, S° . Here, low-temperature heat capacity, C_p , measurements are critical, as they offer the most robust means of determining S° . Low-temperature adiabatic calorimetric heat-capacity measurements have been made in the "Westrum laboratory" on a natural garnet containing about 91% of a grossular component (Westrum et al. 1979) as well as on synthetic grossular (Haselton and Westrum 1980). The resulting S° values given for end-member grossular (i.e., adjusted in the case of the natural sample) are 254.72 ± 0.84 and 260.12 J/(mol·K), respectively. They differ by about 2% and this amount lies outside the error inherent to this precise calorimetric method, which is 0.1 to 0.2% (Robie and Hemingway 1972). There is a third adiabatic calorimetric study that was made on a natural nearly end-member grossular and it gave $S^\circ = 256.48 \pm 1.26$ J/(mol·K)

(Kolesnik et al. 1979). In a fourth calorimetric study, Dachs and Geiger (2006) reinvestigated the same synthetic grossular sample studied by Haselton and Westrum (1980) using low-temperature relaxation calorimetry. They obtained values of $S^\circ = 259.47 \pm 0.25$ and $S^\circ = 257.86 \pm 0.26$ J/(mol·K). The reason(s) for the variations in S° between 254.72 and 260.12 J/(mol·K) is(are) not known. Model-dependent lattice-dynamic-type calculations provide little help in resolving the issue, because they show even larger and smaller S° values of 265 ± 2 (Hofmeister and Chopelas 1991) and 250.1 J/(mol·K) (Pilati et al. 1996), respectively. The standard compilation of calorimetric data on minerals (Robie and Hemingway 1995) lists $S^\circ = 260.12$ J/(mol·K) for grossular. These authors discuss the disagreement in S° values and note that a calorimetric remeasurement of the Haselton and Westrum sample in their lab gave 259.9 J/(mol·K).

In addition to the low-temperature calorimetry studies, the C_p behavior of grossular at $T > 300$ K has also been studied several times. The C_p of various natural and synthetic grossulars was determined by Perkins et al. (1977), Krupka et al. (1979), and Bosenick et al. (1996) using DSC methods up to about 1000 K, with continual improvement in the quality of the data. The data appear to show that the C_p of natural grossular could be slightly less than that of synthetic crystals between about 350 and 700 K (Bosenick et al. 1996). Thiéblot et al. (1999) measured the heat content of synthetic grossular using drop calorimetry between 400 and 1400 K. They summarized the state of knowledge regarding the high-temperature C_p behavior of grossular up to the time of their work. The thermochemical and thermophysical properties of grossular are reviewed and discussed in Geiger (1999).

The calorimetric results show that the heat capacity/entropy of natural grossular crystals, even corrected for deviation from $\text{Ca}_3\text{Al}_2\text{Si}_3\text{O}_{12}$ composition, are different than those measured on synthetic crystals. We stress that in the published works sample characterization, both compositional and structural, can be considered as rudimentary. Chemical and structural differences exist between the various samples and they could, and probably do, affect precise C_p behavior, but little results are available in this regard. To resolve the existing discrepancies, we have undertaken a combined crystal-chemical and calorimetric study of a series of natural and synthetic grossular samples. Our purposes are the following: (1) to review and critically analyze the existing C_p data of grossular; (2) to carefully characterize three synthetic and four natural grossulars to determine their chemical and structural state; (3) to present a set of systematic C_p measure-

ments on the seven different samples; and (4) to derive a new calorimetric-based S° value for grossular and to further reanalyze its standard thermodynamic properties.

SAMPLES AND EXPERIMENTAL METHODS

Synthetic and natural samples

Three different synthetic grossular samples were carefully characterized. All were synthesized at high pressures and temperatures from a glass of grossular composition in piston-cylinder devices in different laboratories. The samples are described in Table 1. Further details regarding the synthesis of the grossular Gr-Has can be found in Haselton (1979) and Haselton and Westrum (1980). The sample, Gr-92, was synthesized at the Bayerisches Geoinstitut using the methods described in Bosenick et al. (1995, 1996). The third synthetic sample, Gr-Kiel, was synthesized at the University of Kiel. All the synthetic samples occur in polycrystalline form.

Four natural grossular samples were also characterized and their locations are described in Table 1. They include two different garnets from the well-known Jeffrey mine locality of Asbestos, Quebec, Canada (Allen and Buseck 1988; Rossman and Aines 1986; Akizuki 1989; Normand and William-Jones 2007), and they have small compositional differences between them. Two other natural samples were also studied. One is light green in color and comes from a locality at Lualenyi, Kenya (Gr-L/K), that is well known for its tsavorite specimens. The locality of the fourth grossular sample (Gr-1/1) is not certain, but based on its appearance and composition (see below) it may also originate from Lualenyi. All the natural garnets occur in single-crystal form, from which small polished platelets were obtained for further study.

Sample characterization

Optical examination. The various grossular samples were examined under a binocular and a polarizing microscope. The single-crystal platelets used for C_p measurement were characterized directly for their optical behavior and the possible presence of inclusions. The polycrystalline synthetic grossulars were examined as grain mounts using an oil with an index of refraction of 1.735.

Microprobe analysis. All grossular samples were examined using back-scattered electron (BSE) images made on an electron microprobe to check for phase purity. Several small single-crystal pieces from the natural garnets and polycrystalline chips from the synthetics were used for measurement. In addition to the BSE measurements, multiple point analyses using line traverses were made to check for compositional zoning and to determine the bulk composition of the samples. The measurements were made using a JEOL microprobe at Kiel University and WDS methods were applied under conditions of 15 kV and 15 nA with a beam size of 1 mm. The standards used for the synthetic samples were corundum for Al, wollastonite for Ca and Si, and a natural fayalite-rich olivine for Fe. For the natural grossulars the above standards were used plus V metal for V, chromite for Cr, tephroite for Mn, rutile for Ti, and forsterite for Mg. The data correction program employed was CITZAF.

X-ray powder diffraction. Two different X-ray powder diffractometers were used. The two synthetic samples Gr-Has and Gr-92 were measured with a Siemens D-500 diffractometer having a graphite secondary monochromator in step-scan mode with $\text{CuK}\alpha$ radiation (40 kV, 35 mA). Gr-Has was measured between 5 and 80 $^\circ 2\theta$ with a step size of 0.02 $^\circ$ with 20 s/step and Gr-92 between

TABLE 1. Description of grossular samples used for study

Sample	Synthesis conditions/locality	Form, color, and optical behavior
Synthetic Gr-Has (Haselton)	Chicago; $T = 1250$ $^\circ\text{C}$, $P = 25$ kbar, 3 h in graphite container	Polycrystalline, grayish white, partly transparent.
Synthetic Gr-92 (Geiger)	Bayreuth; $T = 1250$ $^\circ\text{C}$, $P = 25$ kbar, 12 h in Pt capsule in talc-glass assembly	Polycrystalline, grayish white, partly transparent.
Synthetic Gr-Kiel (Geiger/Demin)	Kiel; $T = 1000$ $^\circ\text{C}$, $P = 16$ kbar, 5 h in Pt capsule in salt assembly	Polycrystalline, grayish white.
Natural Gr; Cat. No. (Gr)-82-112	Jeffrey Mine, Asbestos, Quebec	Single-crystal platelet, colorless and transparent, anisotropic with twinning(?) lamellae. Some alteration(?) material in fractures.
Natural Gr (Hessonite); CMNMC (Gr)-44091	Jeffrey Mine, Asbestos, Quebec	Single-crystal platelet, light pinkish brown, anisotropic wavy extinction, complex zonation. very minor inclusions.
Gr-L/K (Tsavorite?)	Lualenyi, Kenya	Single-crystal platelet, light green, isotropic with very minor fine inclusions.
Gr-1/1	Location not known (Lualenyi, Kenya?)	Single-crystal platelet, very light green, isotropic with no inclusions.

3 and 75 °2 θ with a step size of 0.02° with 10 s/step. The Gr-Kiel sample was measured with an X'Pert MPD diffractometer operating in continuous mode. The measuring conditions were CuK α radiation (40 kV, 40 mA) with a divergence slit of 0.5°, an anti-scatter slit of 0.5°, a receiving slit of 0.35 mm and from 5 to 80 °2 θ with a step size 0.02° and 16 s/step.

MAS NMR spectroscopy. The ²⁹Si MAS NMR spectrum of Gr-Has and the natural grossular, 82-112, and a further synthetic grossular, Gr-35, were measured. Gr-35 was synthesized in a similar manner ($T = 1200$ °C and $P = 20$ kbar from a glass; Bosenick et al. 1995, 1996) as Gr-Has, Gr-92, and Gr-Kiel and its ²⁹Si NMR spectrum was measured over a long spectral range. The ²⁷Al MAS NMR spectrum of Gr-35 was also measured. The experimental setup and measuring conditions are those described in Geiger et al. (1992) and Bosenick et al. (1995). In short, the ²⁹Si spectra were obtained on a 7 mm probe, with 2- μ s, 36° pulses, single pulse excitation, 30 s relaxation delay and spinning speeds of 3 kHz. Between 160 and 2500 transients were accumulated. The ²⁷Al MAS NMR spectrum was measured with a 4 mm probe with spinning speed 8 kHz and $\pi/12$ pulses (=1 μ s). Relaxation delays of 1 s were sufficiently long to prevent saturation. Between 100 and 460 transients were accumulated.

FTIR spectroscopy. FTIR single-crystal spectra were collected on the natural grossular single crystals that were prepared as doubly polished thin crystal platelets with thicknesses between 0.30 and 0.55 mm. The experimental setup is that described in Geiger et al. (2000). Measurements were undertaken in the wavenumber region between 4000 and 350 cm⁻¹ with a Bruker IFS 66V/S FTIR spectrometer equipped with an infrared microscope. An HgCdTe detector, a KBr beam splitter and a SiC source were used in the measurements. The spectral resolution was 4 cm⁻¹ and the beam diameter was fixed between 30 to 70 μ m by setting the crystals on thin metal plates having different aperture sizes. Band positions are considered accurate to ± 2 cm⁻¹.

FTIR powder spectra were collected on the same spectrometer using the KBr pellet technique in the wavenumber region between 4000 and 350 cm⁻¹. Pellets of 13 mm diameter were prepared by pressing a fine mixture consisting of 1 mg of grossular and 200 mg of dried KBr under vacuum. The pellet was kept in a vacuum desiccator for 24 h at 150 °C to minimize any adsorbed water. Spectra were recorded under vacuum with a resolution of 2 cm⁻¹ by combining 512 scans.

Relaxation calorimetric measurements

Low-temperature (i.e., 5–300 K) heat capacity was investigated with the Physical Properties Measurement System (PPMS) constructed by Quantum Design (e.g. Lashley et al. 2003; Dachs and Bertoldi 2005). Heat capacity was measured at 60 different temperatures and three times at each temperature on cooling from 300 K with a logarithmic spacing. A complete PPMS experiment to measure C_p comprises an “addenda run” and a “sample run.” The first measurement determines the heat capacity of the empty sample platform plus Apiezon N grease that facilitates thermal contact between the platform and the sample. In the second measurement, the sample is placed on the platform and the heat capacity of the whole ensemble is measured. The net heat capacity of the sample is then given by the difference between the two measurements. An uncertainty of ± 0.02 mg for the sample weight was adopted for converting the PPMS data from units of μ J·K⁻¹ to units of J/(K·mol).

Measurements on powder samples. The synthetic grossular samples Gr-Has, Gr-R92, and Gr-Kiel were studied. They occur as polycrystalline aggregates.

They were measured using the encapsulation method for powders described in Dachs and Bertoldi (2005), where 19 to 23 mg of sample are sealed in an Al pan so that the powder aggregate is compressed into an ~1 mm thick layer. The samples were not mixed with grease to preserve them for possible further use. The heat capacity of the pans was measured separately and its contribution subtracted from C_p^{total} . As shown by Dachs and Benisek (2011), the accuracy of powder PPMS measurements can be improved by adopting a statistical procedure based on repeated PPMS and differential scanning calorimetry (DSC) measurements. This method permits an accuracy in C_p determinations to better than 1% at temperatures above roughly 50 K and thus allows standard entropy determinations on powder or small crystal aggregates with an accuracy of better than 1%. We used this experimental method here. Three separate PPMS measurements were performed repeating the encapsulation procedure for each determination (Table 2).

Measurements on single crystals. In the case of the natural grossular-rich crystals (Gr-82-112, Gr-44091, Gr-1/1, and Gr-L/K), small, cut and polished platelets were used. This allows them to be directly mounted onto the sample platform for C_p determination. They weighted between 15 and 45 mg. Most measurements were repeated three times to ensure good experimental reproducibility (Table 3). The use of polished single crystals permits better sample coupling (SC) for a PPMS measurement (Dachs et al. 2010). Sample coupling is defined as the ratio $100K_g/(K_g+K_w)$, where K_g is the thermal conductance between the sample and the sample platform and K_w is the thermal conductance of the wires that attach the sample platform to the puck frame (see Hwang et al. 1997; Lashley et al. 2003; Dachs and Bertoldi 2005 for more details). The closer the sample coupling is to 100%, the better the thermal conductance between the sample platform and the sample, which ensures a more robust heat-capacity determination. The associated experimental C_p accuracy is better than 0.5% above ~50 K and is about the same for a standard entropy determination (Dachs et al. 2010).

DSC measurements

Heat capacity between 282 and 764 K was measured with a Perkin Elmer Diamond DSC using Perkin Elmer Al pans and lids, with the former containing a loose polycrystalline powder or a single-crystal platelet. Each C_p determination consists of three separate measurements of a blank, a reference and a sample measurement. Before every sample measurement, the DSC was calibrated with a reference run using a synthetic single crystal of corundum (31.764 mg). Its heat-capacity values were taken from a National Bureau of Standards Certificate (Ditmars et al. 1982). Each garnet sample was measured three to four times in this manner. The mean and standard deviation of these data are averaged to obtain C_p and σ_{C_p} for one experimental series. The mean relative uncertainties are $\sim 0.25\%$ for C_p in the range $300 < T < 600$ K and $\sim 0.35\%$ at $T > 600$ K. Three different DSC mounts for each synthetic grossular were prepared to obtain three independent DSC data sets per sample. The experimental method is similar to that used for the PPMS powder measurements.

The DSC measurements were performed under a flow of Ar gas and the calorimeter block was kept at a constant temperature of 243.3 K using a Perkin Elmer Intracooler. A flow of dried air prevented the growth of ice crystals on the calorimeter block (the flow was set to 200 mL/min and the cover heater was turned off). The heat-flow data were collected in the step-scanning mode with a heating rate of 10 K/min in temperature intervals of 100 K. The heat capacity of the blank run was subtracted from that of the reference and sample measurement,

TABLE 2. Experimental parameters for PPMS and DSC heat-capacity measurements on synthetic grossular samples

Sample			PPMS					DSC			S° PPMS [J/(mol·K)]	S° DSC adjusted [J/(mol·K)]	Difference from literature	
	Formula weight (g/mol)	Sample weight (mg)	SC* 5 K (%)	SC* Max (%)	SC* 300 K (%)	C [†] /C ^{add†} 5 K (%)	C [†] /C ^{add†} 300 K (%)	Sample mass (mg)	n‡	Factor§ Min Max				
Gr-Has	1	450.454	22.34	95.6	99.8	99.7	0.02	0.27	28.27	3	0.995	261.5 \pm 2.0	260.9 \pm 2.0	+0.3
	2		21.97	96.5	99.8	99.5	0.03	0.27	27.05	3	1.006	260.2 \pm 2.0		
	3		22.72	92.4	99.9	99.7	0.02	0.28	26.78	3		261.3 \pm 2.0		
Gr-R92	1	450.454	21.02	98.5	99.8	99.6	0.02	0.26	24.37	3	0.996	259.5 \pm 2.1	259.1 \pm 2.2	-0.4
	2		19.42	97.4	99.9	99.7	0.02	0.24	23.32	3	1.003	259.4 \pm 2.3		
	3		20.27	91.7	99.9	99.7	0.02	0.25	22.44	3		258.4 \pm 2.2		
Gr-Kiel	1	450.454	23.30	98.6	99.8	99.6	0.02	0.29	26.71	3	1.000	258.7 \pm 1.9	260.4 \pm 2.0	+0.1
	2		23.00	98.4	99.8	99.6	0.03	0.28	23.80	3	1.005	260.1 \pm 2.0		
	3		21.97	95.3	99.8	99.6	0.03	0.27	23.30	4		259.6 \pm 2.0		

* SC: Sample coupling (see text for details). 5 K: Value at 5 K (mostly minimum); Max: Maximum value; 300 K: Value at 300 K.

† C[†]/C^{add†}: ratio of sample over addenda heat capacity at 5 and 300 K.

‡ n = number of DSC measurements for each series.

§ Factor for adjusting the PPMS data, i.e., $(C_p^{\text{DSC}}/C_p^{\text{PPMS}})_{\text{at } 298 \text{ K}}$ as in Equation 1. Minimum and maximum values are given.

|| $100(S^{\circ}_{\text{this study}} - S^{\circ}_{\text{literature}})/S^{\circ}_{\text{literature}}$. The literature value is $S^{\circ} = 260.12$ J/(mol·K) as taken from Haselton and Westrum (1980).

respectively, following the method described in Mraw (1988), using a self-written Mathematica program. The final accuracy of our C_p data is better than 0.6% applying this experimental procedure and the described DSC instrumental settings (Dachs and Benisek 2011).

Data evaluation

The low- T C_p data of the three different synthetic grossulars were adjusted according to the relationship

$$(C_p^{\text{PPMS}})_{\text{adjusted}} = (C_p^{\text{PPMS}})_{\text{measured}} (C_p^{\text{DSC}}/C_p^{\text{PPMS}})^{298\text{ K}}. \quad (1)$$

This relationship is derived using the three independently measured PPMS and DSC heat-capacity data sets where they overlap around ambient temperature. Equation 1 has a value of unity, if the C_p values for the two sets are the same (Dachs and Benisek 2011). The application of Equation 1 to all possible combinations of the three PPMS and three DSC heat capacity data sets results in nine adjusted C_p data series per sample. The mean C_p values from them were taken to give the C_p behavior for each sample. Last, the C_p results for each synthetic sample were averaged to produce one final C_p data set for end-member grossular. We note that there was no overt reason, a priori, to prefer one grossular sample to another.

The standard molar entropy, S° , at 298.15 K was calculated from this final averaged C_p data set by numerically solving the integral

$$S^\circ - S^{T=0\text{ K}} = \int_0^{298.15} \frac{C_p}{T} dT \quad (2)$$

assuming $S^{T=0\text{ K}} = 0$ and using the Mathematica functions *NIntegrate* and *Interpolation* for linear interpolation between data points. The integral was evaluated over the range 5 to 298.15 K and the entropy increment from 0 to 5 K was ignored. The uncertainty in S° was calculated according to Benisek and Dachs (2008).

Smoothed thermodynamic functions for “pure end-member” grossular were calculated by fitting the final C_p data set, consisting of the three synthetic grossulars, and including five DSC data points between 282 and 300 K. This was done using an empirical equation (see Boerio-Goates et al. 2002; Dachs et al. 2009)

$$C_p = 3R[n \cdot D(\theta_D) + m \cdot E(\theta_E) + n_s \cdot S(\theta_s)], \quad (3)$$

where $D(\theta_D)$, $E(\theta_E)$, and $S(\theta_s)$ are Debye, Einstein, and Schottky functions (DES), respectively, and m , n , n_s , θ_D , θ_E , and θ_s are adjustable parameters (Supplementary Table 1¹). For an optimal representation of the low- T heat-capacity behavior, the data were divided into low- and high-temperature intervals. Thus, two sets of fit parameters are obtained and are used below and above T^{switch} , respectively. Applying Equations 3 and 2 to account for the entropy increment from 0 to 5 K amounts to only 0.005 J/(mol·K) for grossular. It can, therefore, be neglected for the entropy values that were obtained by numerical integration.

RESULTS

Sample description and optical examination

The three synthetic grossulars occur as fine-grained polycrystalline chips with individual grain sizes varying between about 5 and 20 μm . The individual crystals of the Gr-Kiel sample are small, about 5–10 μm in diameter, and they are isotropic under crossed polarizers. Very minor amounts (i.e., <1%) of anisotropic impurities are observed. The other two samples Gr-Has and Gr-92 show slightly different optical behavior. Here, crystals appear to be slightly larger and they sometimes show a very weak anisotropy, which tends to be most pronounced at the grain boundaries. It is also possible to see at high magnification very minute elongated crystals in their grain mounts. Due to their minute size the very fine crystals could not be identified optically. It is difficult to determine if the observed anisotropy on some crystals rims is related to the crystals themselves or is due to some type of complex light scattering process arising from grain boundaries in the

polycrystalline aggregates.

The natural grossular samples from the Jeffrey mine are optically complex and notably anisotropic. The sample CMNMC 44091 is similar optically to the orange garnets described by Akizuki (1989) from the same locality. Under crossed polarizers one can observe patterns of lamellae, which Akizuki suggests could be twins (Supplementary Fig. 1a¹; see also Figs. 2a and 3 in Akizuki 1989). The sample 82-112 shows, somewhat in contrast, a complex more irregular anisotropic behavior (Supplementary Fig. 1b¹; see also Fig. 4 in Akizuki 1989). In both samples, parts of some crystals showed small amounts of birefringent inclusions consisting of other solid phases. They were removed in the case of the crystal platelets that were investigated calorimetrically. The two natural garnets Gr-1-1 and Gr-L/K are, in contrast to those from the Jeffrey mine, optically isotropic (Supplementary Fig. 1c¹) and 99% inclusion free. The optical observations are summarized in Table 1.

Microprobe analysis

The BSE images proved useful in checking for the presence of fine solid-phase inclusions <10 μm in size. The results show that the four natural grossulars were largely inclusion free. The crystals also show no major compositional zonation. The synthetic grossular of Haselton and Westrum (1980), on the other hand, shows what appear to be very fine needle-like crystals in some polycrystalline chips (Supplementary Figs. 2a and 2b¹). Due to their very fine grain size, it was not possible to obtain an interpretable chemical analysis of them. Apparently, the results represent a complex mixture of the inclusion phase and grossular. The other two synthetic grossulars (Gr-92 and Gr-Kiel) did not reveal, in spite of the X-ray results (see below), the presence of any phase other than garnet (Supplementary Figs. 2a and 2b¹).

The average compositions for all grossular samples, based on about 30 to 40 point analyses made using line traverses, are given in Supplementary Table 2¹. It appears that the two synthetic samples Gr-Has and Gr-92 show small deviations from exact grossular stoichiometry. In several point analyses on Gr-Has the stoichiometric value for Si is too low, while the number of Al atoms is too high. The crystal-chemical formulas for the four natural grossulars, broken down into various end-member garnet components, were calculated using the program of Locock (2008) and are given in Table 4. It was assumed in the calculation that all H₂O was held in the katoite-type (i.e., hydrogrossular) substitution (see below).

X-ray powder diffraction

An X-ray powder diffractogram of the synthetic grossular Gr-Has is shown in Supplementary Figure 3¹. The diffractograms of other two synthetic samples are similar. All patterns show strong and narrow reflections from grossular indicating

¹ Deposit item AM-12-059: CIFs, Appendices 1 and 2, Supplementary Tables 1–3, and Figures 1, 2, 3, 9, 15, 16, and 17. Deposit items are available two ways: For a paper copy contact the Business Office of the Mineralogical Society of America (see inside front cover of recent issue) for price information. For an electronic copy visit the MSA web site at <http://www.minsocam.org>, go to the *American Mineralogist* Contents, find the table of contents for the specific volume/issue wanted, and then click on the deposit link there.

good crystallinity. They also show several very weak peaks that are best indexed to wollastonite or to a wollastonite-like phase. Based on the relative peak heights of wollastonite and garnet reflections, we estimate roughly 1–2 volume percent of the former in all samples, with the Gr-Kiel sample showing the least amount of wollastonite. This sample also contains a very minor amount of NaCl. The Gr-Has and Gr-92 samples also show about two or three other very weak reflections that could not be assigned.

MAS NMR spectroscopy

The ^{29}Si MAS NMR spectra of synthetic grossulars Gr-Has and Gr-35 and the natural grossular Gr-82-112 from the Asbestos mine are shown in Figure 4. Both synthetic samples show a single, narrow resonance centered at -83.9 ppm (see Bosenick et al. 1995). The single resonance in the spectrum of Gr-82-112 is also at -83.9 ppm, but it is considerably broadened. This is attributed to the presence of paramagnetic Fe and similar behavior has been noted before in both natural and synthetic grossular-pyrope garnets (Geiger et al. 1992; Kelsey et al. 2008). The ^{27}Al NMR spectrum of Gr-35 (Fig. 5) shows a resonance with typical quadrupole broadening deriving from Al in octahedral coordination. No additional resonances can be observed in the NMR spectra.

FTIR spectroscopy

The FTIR single-crystal spectra of the four natural grossular samples in the wavenumber region from 4000 to 3000 cm^{-1} are shown in Figure 6. The spectra are, in general, relatively complex and no specific OH mode assignments can be made. Rossman and Aines (1991) undertook an IR study on a large number of grossular-hydrogrossular garnets to document the systematics of the OH bands in such garnets, and we compare our results to theirs. The spectrum of the colorless Jeffrey mine grossular Gr-82-112 is similar in appearance to the Rossman and Aines (1989) spectra of samples 1051 and 941. The strongest IR band in the spectrum of sample Gr-82-112 is located at 3612 cm^{-1} . The spectrum of the light pinkish-brown Jeffrey mine sample Gr-44091 shows more bands and is un-

like any spectrum shown in Rossman and Aines (1991). The most intense band is located at 3630 cm^{-1} . The spectrum of this sample appears also to show a very weak broad H_2O band located roughly at 3420 cm^{-1} , which may be due to very minute fluid inclusions that are not visible optically. The spectrum of Gr-L/K is similar in appearance to the Class 2, grossular 771 from Meralini Hills, Tanzania (Rossman and Aines 1991), and its three strongest bands are located at 3642 , 3600 , and 3565 cm^{-1} . The spectrum of sample Gr-1/1 is similar to that of Gr-L/K, the only significant difference being in the relative intensity of certain OH bands but not their energies.

The various spectra studied here are more complex than that of hydrogrossular (katoite) and hydrogrossular-containing garnets, that is, those with an $\text{O}_4\text{H}_4 \leftrightarrow \text{SiO}_4$ substitution (Rossman and Aines 1991; Kolesov and Geiger 2005). It is probable that OH is incorporated in our natural garnets via several structural mechanisms. The amount of total H_2O can be estimated using the results of Rossman and Aines (1991) giving ~ 0.3 and $0.2\text{ wt}\%$ H_2O for the samples from Asbestos and Kenya, respectively.

The IR powder spectra in the region between 1200 to 350 cm^{-1} are shown in Figure 7. In this wavenumber region various lattice vibrations are present. The spectra are consistent with the spectra of synthetic grossular presented in Geiger (1998), Bosenick et al. (1995), and Boffa Ballaran et al. (1999). The absorption bands are generally similar in wavenumber and intensity for all samples both synthetic and natural. Small spectral differences can be observed, though, between some samples. The most notable feature, for example, involves the band doublet centered at about 850 cm^{-1} , where both modes are assigned to ν_3 vibrations of the SiO_4 groups. In the case of the synthetic Gr-Has and the natural sample Gr-82-112, it can be observed that this doublet is slightly broadened. Its low-energy flank sweeps out to lower energies and the two bands of the doublet show similar intensity compared to this doublet in the spectra of the other grossular samples (Fig. 7). This could, perhaps, be related to the presence of a small underlying band(s) due to another phase or possibly slight cation order/disorder effects (see below). In the spectra of the other samples this doublet is

TABLE 3. Experimental parameters for PPMS and DSC measurements on natural grossular single crystals

Sample	X_{Gr}^*	Formula weight (g/mol)	Sample weight (mg)	PPMS			$C^{\ddagger}/C^{\text{add}\ddagger}$ 5 K	$C^{\ddagger}/C^{\text{add}\ddagger}$ 300 K	PPMS/DSC agreement at 298 K§	S° PPMS [J/(mol·K)]	S° mean [J/(mol·K)]	S° corrected to end-member [J/(mol·K)]
				SC† Min (%)	SC† Max (%)	SC† 300 K (%)						
Gr-82-112	0.971	452.168	29.49	96.4	99.8	99.5	1.08	2.48	-0.34	258.0 ± 1.0	258.1 ± 1.0	255.1 ± 1.2
				97.5	99.9	99.7	1.52	2.59	-0.61	258.3 ± 1.0		
				96.6	99.9	99.8	1.41	2.58	-0.43	258.1 ± 1.0		
Gr-44091	0.940	454.744	37.58	99.1	100	99.1	1.57	3.26	-0.60	261.1 ± 1.0	261.1 ± 1.0	255.2 ± 1.2
				99.2	99.9	99.3	1.12	3.12	-0.64	260.9 ± 1.0		
				99.1	99.9	99.3	1.50	3.23	-0.50	261.2 ± 1.0		
Gr-1/1	0.944	451.795	30.68	99.0	100	99.6	1.20	2.63	-0.70	258.0 ± 1.0	258.0 ± 1.0	253.6 ± 1.2
				98.2	100	99.5	1.12	2.61	-0.67	258.0 ± 1.0		
				98.5	100	99.5	1.44	2.70	-0.62	258.0 ± 1.0		
Gr-L/K	0.937	450.208	14.98	90.4	100	100	0.66	1.32	+0.22	257.7 ± 1.1	257.2 ± 1.1	253.0 ± 1.2
				94.6	100	100	0.54	1.29	-0.11	256.8 ± 1.1		
				94.6	100	99.6	0.60	1.30	-0.13	257.1 ± 1.0		
				99.0	99.8	99.5	1.63	3.89	-0.28	257.2 ± 1.1		

Notes: Number of DSC measurements for each sample is three.

* Mole fraction of the grossular component. Garnet compositions are given in Table 4.

† SC: Sample coupling. Min: Minimum value; Max: Maximum value; 300 K: Value at 300 K.

‡ $C^{\ddagger}/C^{\text{add}\ddagger}$: ratio of sample over addenda heat capacity at 5 and 300 K.

§ $100(C_p^{\text{PPMS}} - C_p^{\text{DSC}})/C_p^{\text{DSC}}$ at 298 K.

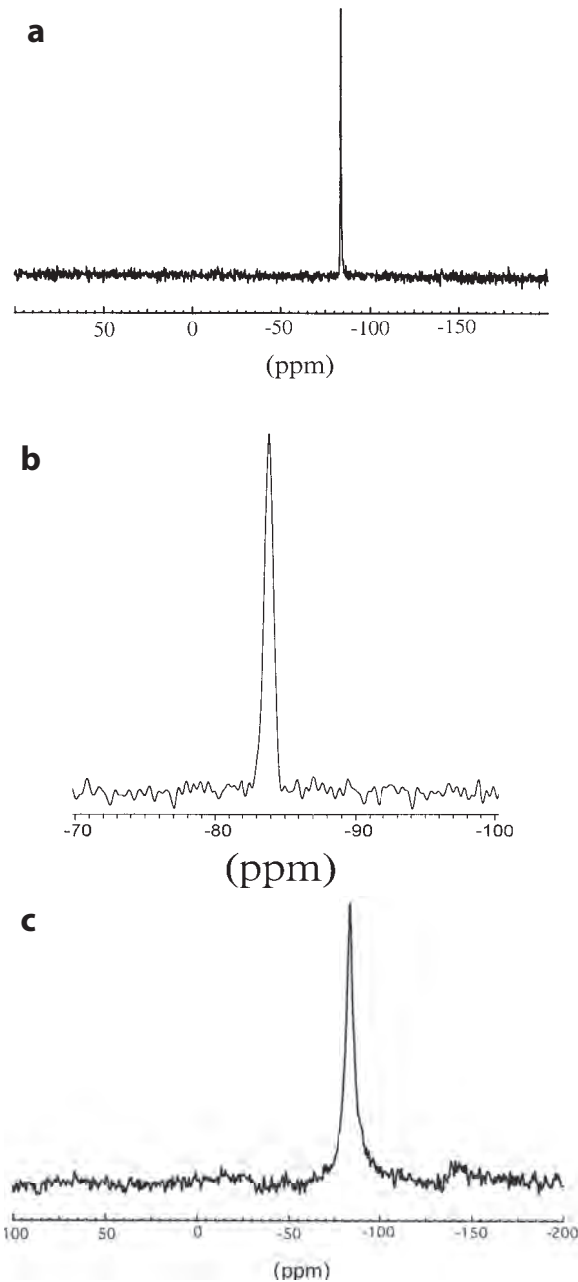


FIGURE 4. ^{29}Si MAS NMR spectrum of grossular. (a) spectrum of sample Gr-35 between 100 and -200 ppm showing a single resonance at -83.9 ppm, (b) spectrum of sample Gr-Has between -70 and -100 ppm showing a single resonance at -83.9 ppm, (c) spectrum of natural grossular, Gr-82-112, between 100 and -200 ppm showing a broadened resonance at -83.9 ppm.

narrower and the higher energy band is slightly more intense compared to the lower energy band.

Low-temperature heat capacity behavior of synthetic grossular

The raw C_p data for the three synthetic polycrystalline grossular samples are given in Appendix 1 of the Supplementary

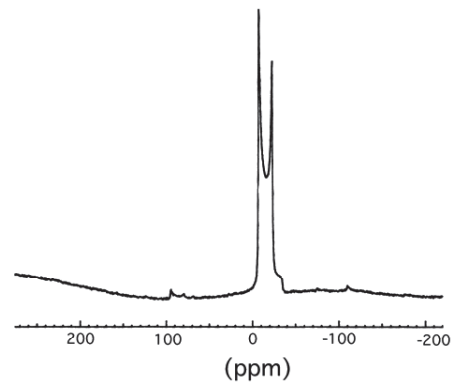


FIGURE 5. ^{27}Al MAS NMR spectrum of sample Gr-35 between 250 and -200 ppm.

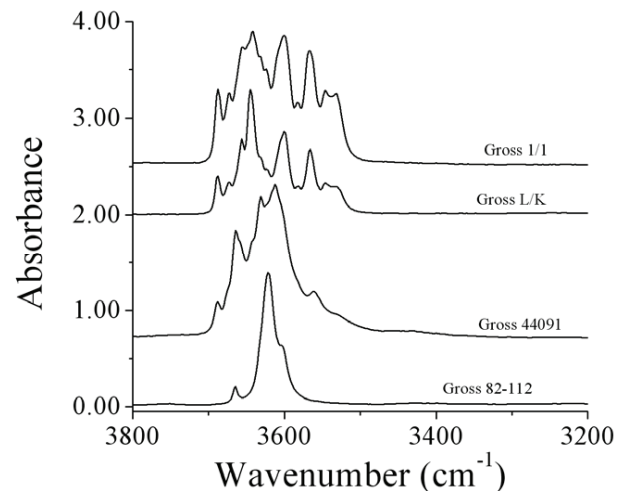


FIGURE 6. FTIR single-crystal spectra of the various natural grossular samples in the wavenumber region from 3800 and 3200 cm^{-1} . The various bands represent OH vibration whose exact assignment is not possible to make. The most intense bands are located at: 3620 cm^{-1} for grossular sample 82-112; 3613 cm^{-1} for Gr-44091; 3642 , 3600 , and 3565 cm^{-1} for Gr-L/K; and 3640 , 3600 , and 3565 cm^{-1} for Gr-1/1.

information¹ and shown in Figure 8. Table 2 lists the experimental details of the PPMS and DSC measurements. Sample coupling lies in the range 99.5 to 99.7% at 300 K for all measurements. It typically shows a maximum of 99.8 to 99.9% in the temperature range 100 to 200 K and decreases continuously to between 98.6 and 91.7% at 5 K (Table 2).

The adjustment factors ($C_p^{\text{DSC}}/C_p^{\text{PPMS}})^{298\text{K}}$ from Equation 1 lie in the range 0.995 to 1.006 (Table 2) demonstrating that PPMS and DSC heat capacity values differ by not more than $\pm 0.6\%$, where they overlap around ambient temperature (Fig. 8). The relative differences between our adjusted heat-capacity values compared to the low-TAC data of Haselton and Westrum (1980) are shown in Supplementary Figure 9a¹ for each synthetic grossular sample and in Supplementary Figure 9b¹ for the final averaged C_p data set. Above ~ 50 K, the agreement is mostly better than 1%. At low

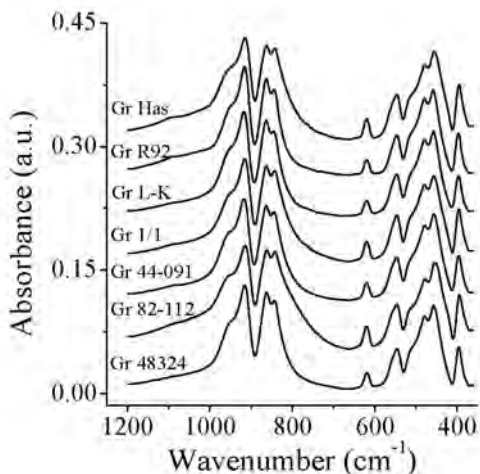


FIGURE 7. FTIR powder spectra of grossular samples in the wavenumber region from 1250 to 350 cm^{-1} showing various lattice modes. The modes between 1000 and 700 cm^{-1} are internal stretching modes of the SiO_4 tetrahedra and those at lower wavenumbers can be assigned to various external “lattice vibrations.”

temperatures, relative differences are greater being up to ~20% at ~5 K. These deviations are largely within the 1σ -uncertainty envelope of the PPMS data (Supplementary Fig. 9b¹). The larger experimental imprecision in the PPMS method at low T is related to an unfavorable sample to addenda heat-capacity ratio (e.g., Lashley et al. 2003). At very low temperatures, only a few percent of the total measured heat capacity originates from grossular (Table 2).

Standard entropy of synthetic grossular

The individual standard-entropy values for each PPMS measurement for the three synthetic grossular samples are listed in Table 2. They range between 260.2 to 261.5 $\text{J}/(\text{mol}\cdot\text{K})$ for Gr-Has, 258.4 to 259.5 $\text{J}/(\text{mol}\cdot\text{K})$ for Gr-R92, and 258.7 to 260.1 $\text{J}/(\text{mol}\cdot\text{K})$ for Gr-Kiel. The scatter in S° for a given sample is always less than the 1σ uncertainty calculated according to Benisek and Dachs (2008), which is ± 1.9 to 2.3 $\text{J}/(\text{mol}\cdot\text{K})$. This demonstrates a good reproducibility for our experimental

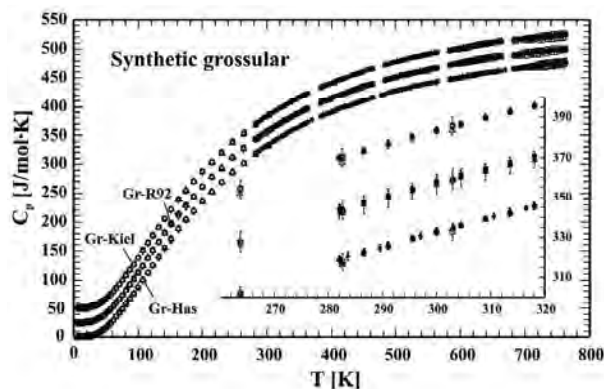


FIGURE 8. Heat capacity values for the synthetic grossular samples Gr-Has, Gr-R92, and Gr-Kiel as a function of temperature. Note that the C_p values of Gr-R92 and Gr-Kiel are offset by +25 and +50 $\text{J}/(\text{mol}\cdot\text{K})$ to avoid overlap. Open symbols represent the PPMS measurements (the mean of the three PPMS C_p determinations at each temperature is plotted) and the filled symbols the DSC data. The overlapping region between PPMS and DSC data is shown in the inset. Error bars represent 2σ and are for the PPMS measurements only shown in the inset.

method. The final DSC-adjusted C_p values yield $S^\circ = 260.9 \pm 2.0 \text{ J}/(\text{mol}\cdot\text{K})$ for Gr-Has, $S^\circ = 259.1 \pm 2.2 \text{ J}/(\text{mol}\cdot\text{K})$ for Gr-R92, and $S^\circ = 260.4 \pm 2.0 \text{ J}/(\text{mol}\cdot\text{K})$ for Gr-Kiel. Our recommended S° calorimetric value for end-member grossular is thus $260.23 \pm 2.10 \text{ J}/(\text{mol}\cdot\text{K})$, as given by the average of the former three values. This is in excellent agreement with the low-TAC value of 260.12 $\text{J}/(\text{mol}\cdot\text{K})$ given by Haselton and Westrum (1980) using adiabatic calorimetry. Smoothed values for the various thermodynamic functions in Supplementary Table 1¹ for synthetic grossular were calculated with the parameters listed in Supplementary Table 3¹ from a fit of the final C_p data set to Equation 3.

It is important to note that the experimental scatter and uncertainty in the PPMS data at $T < 50 \text{ K}$ have little effect on the determined standard entropy value. This is because the entropy increment from 0 to 50 K is only 5.41 $\text{J}/(\text{mol}\cdot\text{K})$, which amounts to just 2.1% of S° . If one takes, alternatively, the Haselton and Westrum C_p data as “correct” and which are ~3 to ~10% lower between 10 and 40 K (Supplementary Fig. 9b¹), the correspond-

TABLE 4. Crystal-chemical formulas of natural grossulars calculated using the program of Locock (2008)

End-member	Formula	Gr-82-112	Gr-40091	Gr-1/1	Gr-L/K	Thetford*	Bazhenovo Intrusion Ural† - 1	Bazhenovo Intrusion Ural† - 2
Henritermierite	$\{\text{Ca}_3\}[\text{Mn}_2](\text{SiO}_3)_2(\text{OH})_4$	0.07%		0.59%	0.20%			
Katoite	$\{\text{Ca}_3\}[\text{Al}_2](\text{OH})_{12}$	1.22%	1.25%	0.64%	0.77%	0.80%		0.83%
Schorlomite-Al	$\{\text{Ca}_3\}[\text{Ti}_2](\text{SiAl})\text{O}_{12}$	0.03%	0.17%	1.13%	0.83%	0.68%		
Morimotoite-Mg	$\{\text{Ca}_3\}[\text{TiMg}](\text{Si}_3)\text{O}_{12}$			0.50%	0.70%			
Morimotoite	$\{\text{Ca}_3\}[\text{TiFe}](\text{Si}_3)\text{O}_{12}$					0.07%		
Goldmanite	$\{\text{Ca}_3\}[\text{V}_2](\text{Si}_3)\text{O}_{12}$	0.12%	0.09%	0.27%	0.87%			
Uvarovite	$\{\text{Ca}_3\}[\text{Cr}_2](\text{Si}_3)\text{O}_{12}$	0.03%	0.03%	0.03%	0.09%		0.06%	
Spessartine	$\{\text{Mn}_3\}[\text{Al}_2](\text{Si}_3)\text{O}_{12}$	0.12%	1.38%	0.35%	1.03%	1.39%	0.21%	0.21%
Pyrope	$\{\text{Mg}_3\}[\text{Al}_2](\text{Si}_3)\text{O}_{12}$	0.11%	0.07%	1.10%	1.55%	0.90%		
Almandine	$\{\text{Fe}_3\}[\text{Al}_2](\text{Si}_3)\text{O}_{12}$		2.22%			1.89%		
Grossular	$\{\text{Ca}_3\}[\text{Al}_2](\text{Si}_3)\text{O}_{12}$	97.14%	94.04%	94.38%	93.74%	91.43%	97.01%	94.98%
Andradite	$\{\text{Ca}_3\}[\text{Fe}_2](\text{Si}_3)\text{O}_{12}$	1.08%	0.51%	1.00%	0.22%	2.85%	2.00%	0.85%
Remainder		0.08%	0.24%	0.00%	0.00%	0.00%	0.72%	3.13%
Total		100.00%	100.00%	99.99%	100.00%	100.01%	100.00%	100.00%

* Oxide weight percents taken from Westrum et al. (1979).

† Oxide weight percents taken from Kolesnik et al. (1979) from their analyses 1 and 2 assuming only Fe_2O_3 .

ing entropy for this temperature segment is 5.23 J/(mol·K). Thus, any possible experimental error in the PPMS measurements at low temperatures could only affect the S° value <0.1%.

High-temperature heat capacity behavior of synthetic grossular

The DSC data for the three synthetic grossular samples are compiled in Appendix 1¹ (Supplementary information) that lists the mean C_p values and standard deviation of the repeated measurements. The nine DSC series, consisting of three determinations per sample, where each, in turn, represents a mean of three to four separate measurements (Table 2), were averaged to obtain a final single high-temperature C_p data set. These data show a precision of $0.20 \pm 0.05\%$ at $300 < T < 600$ K and $0.3 \pm 0.1\%$ at $T > 600$ K. The results are shown in Figures 10a and 10b together with other published C_p data for synthetic grossular, namely from the DSC studies of Bosenick et al. (1996) and Krupka et al. (1979) and from the adiabatic calorimetry study of Haselton and Westrum (1980). Our C_p data are in excellent agreement with those of Bosenick et al. (1996), who measured a grossular sample up to 972 K that was synthesized similarly to those studied here. Both C_p data sets are very similar between about 300 and 650 K with relative differences of <0.5%. At high temperatures there

is a difference of ~ 2.5 J/(mol·K) between our and their data (Fig. 10b). We refrained from combining our DSC data with those measured by Bosenick et al. (1996) above 764 K for the purpose of fitting a C_p polynomial, although both sets overlap within 2σ uncertainty. None of the DSC data of Krupka et al. (1979) were considered further, because of their large scatter and their clear deviations from the more recent measurements of Bosenick et al. (1996) and this work.

For fitting a C_p polynomial, we combined the three highest temperature PPMS C_p data with the final averaged DSC data set. We also used the relative enthalpy values measured by Thiéblot et al. (1999) on a synthetic grossular using drop calorimetry between 408 and 1350 K to constrain the C_p polynomial at high temperatures. These later data have an experimental uncertainty of <0.2%, excepting the highest T datum at 1386 K, which suffered from experimental problems (Thiéblot et al. 1999, their Table 2). Adopting the C_p polynomial of Berman and Brown (1985) and applying the method of least-squares yields in J/(mol·K)

$$C_p = 556.18(\pm 12) - 1289.97(\pm 394) \cdot T^{-0.5} - 2.44014(\pm 0.24) \cdot 10^7 \cdot T^{-2} + 3.30386(\pm 0.39) \cdot 10^9 \cdot T^{-3}. \quad (4)$$

This polynomial (Figs. 10a and 10b) fits the DSC data with a deviation of <0.2%. A value of $C_p^{298} = 331.63$ J/(mol·K) is calculated, which is only 0.15% larger than $C_p^{298} = 331.12$ J/(mol·K) resulting from the DES fit from Equation 3. Figure 11a shows the C_p behavior of grossular from 300 to 2000 K as calculated from Equation 4. It can be compared to C_p values calculated with polynomials presented in Bosenick et al. (1996), from various thermodynamic databases (Berman 1988; Gottschalk 1997; Chatterjee et al. 1998; Holland and Powell 1998, 2011) and from that calculated using vibrational spectra (Chopelas 2006). Figure 11b is a percent difference plot, given as $100[(C_p^{\text{Eq.4}} - C_p^{\text{ref}})/C_p^{\text{ref}}]$ as a function of temperature. Agreement between calculated C_p values from the various polynomials is generally better than $\sim 1\%$ up to ~ 1000 K and published polynomials give heat capacities that are smaller by up to this amount below this approximate temperature. Above ~ 1000 K, the behavior of the various C_p polynomials is reversed, and they give larger values, with relative differences reaching 5% at 2000 K. An exception is the Chatterjee et al. (1998) polynomial that yields from 300 to 2000 K smaller C_p values throughout compared to Equation 4. We also note, as did Thiéblot et al. (1999), that the C_p values of Haselton and Westrum (1980) above ~ 300 K tend to be slightly greater than those of Thiéblot et al. (1999) and from this study. The highest temperature data of Haselton and Westrum appear to “run” slightly with temperature. At 350 K, their C_p data are up to $\sim 1.4\%$ larger than our DSC-based results (Figs. 10 and 11b). It is possible that a slight heat leak was an issue in their adiabatic calorimetry measurements at $T > 300$ K, which leads to their larger C_p values in this range (see Dachs et al. 2012, for a further discussion on this subject).

Figure 12 shows a plot of the difference in calculated relative enthalpy values for grossular vs. those measured by Thiéblot et al. (1999). Relative enthalpy values, calculated using Equation 4 and using the C_p polynomial of Bosenick

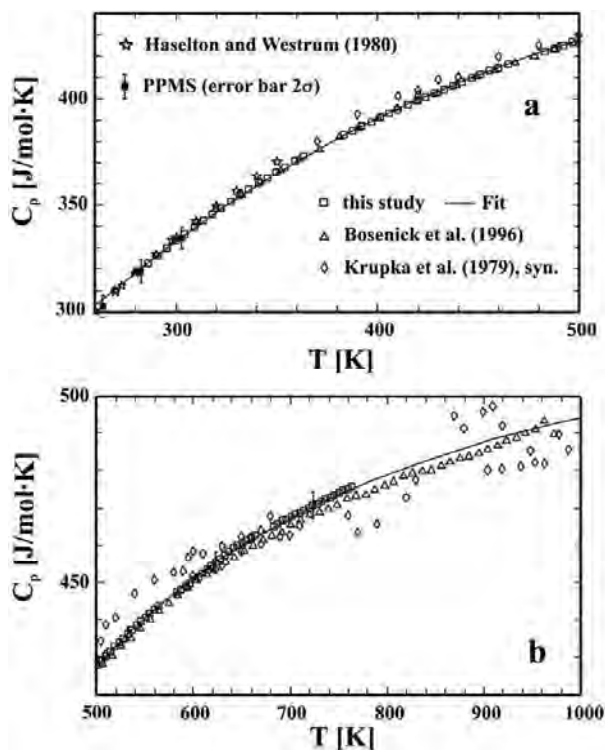


FIGURE 10. DSC heat capacity values from this study compared to those from other studies on synthetic grossular (a) between 280 and 500 K and (b) between 500 and 1000 K. The solid line is the best-fit polynomial according to Equation 4 using the final averaged DSC data set (squares). The data of Haselton and Westrum (1980), measured by adiabatic calorimetry in the range 280 to 350 K, and the highest temperature PPMS data are also shown in a.

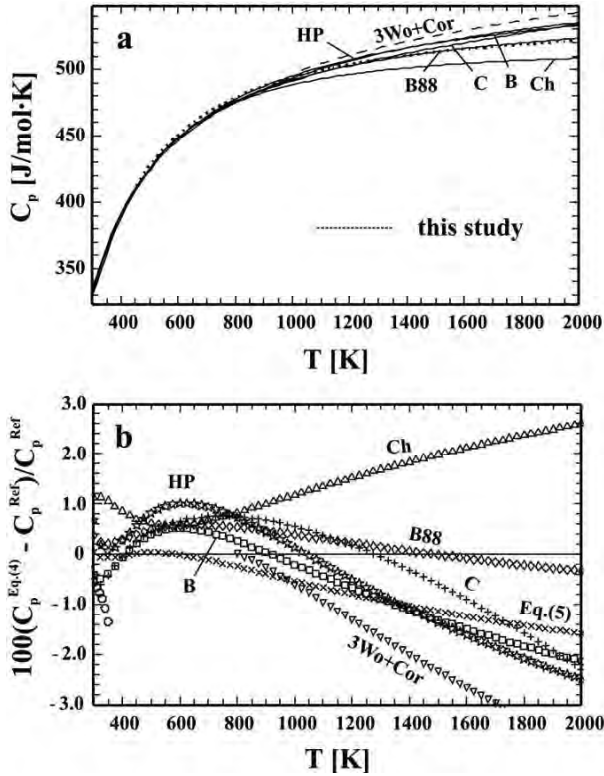


FIGURE 11. (a) Heat capacity of grossular from 300 to 2000 K from various published C_p polynomials or from modeling of vibrational spectra. Curves labeled as B88 (Berman 1988), B (Bosenick et al. 1996), C (Chopelas 2006), Ch (Chatterjee et al. 1998), HP (Holland and Powell 1998, 2011). The short-dashed line is from Equation 4 of this study and the long-dashed line is based on the approximation $3C_p^{\text{wollastonite}} + C_p^{\text{corundum}}$ using the HP data set, (b) Percent difference plot for the C_p behavior from this study ($C_p^{\text{Eq.4}}$) compared to other results (C_p^{Ref}): B88 (diamonds), B (squares), C (crosses), Ch (triangles), and HP (stars). X symbols represent the percent difference for C_p values calculated using Equation 4 and Equation 5, the inverted triangles the approximation $3C_p^{\text{wollastonite}} + C_p^{\text{corundum}}$ and the circles the C_p data from Haselton and Westrum (1980).

et al. (1996), fall largely within a $\pm 0.2\%$ error band of the experimental data. The C_p polynomials of Holland and Powell (1998, 2011), Berman (1988), and Chatterjee et al. (1998) lead to relative enthalpy values that are not as in good agreement with the experimental data. The Chatterjee et al. polynomial gives values that are consistently too low by about 1% at all temperatures. The polynomials of Holland and Powell (1998, 2011) and Berman (1988) represent the data slightly better, but they also give values outside the error of $\pm 0.2\%$ associated with drop calorimetry. In the case of the Berman (1988) data set, the reason for the poor agreement is that the DSC data of Perkins et al. (1977) from 600 to 1000 K were used for deriving a C_p polynomial. These C_p measurements were made on a natural grossular sample, which generally gives slightly lower C_p values compared to synthetics. Holland and Powell (1998) used estimated coefficients for their C_p polynomial. The same set of coefficients appears in Holland and Powell (2011), although

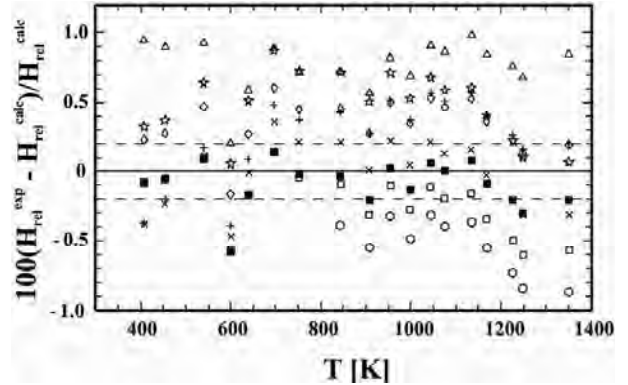


FIGURE 12. Percent difference plot for the relative enthalpies measured by Thiéblot et al. (1999) on synthetic grossular using drop calorimetry (H_{rel}^{exp}) and calculated values (H_{rel}^{calc}). Dashed lines represent an experimental error of $\pm 0.2\%$. The various symbols and sources are: open squares Equation 4 of this study; filled squares Equation 5 of this study; X symbol = Bosenick et al. (1996); triangles = Chatterjee et al. (1998); diamonds = Berman (1988); stars = Holland and Powell (1998, 2011 = HP); crosses = Chopelas (2006); and the hexagons represent the approximation $C_p^{\text{grossular}} = 3C_p^{\text{wollastonite}} + C_p^{\text{corundum}}$ as based on the HP data set.

Bosenick et al. (1996) and Thiéblot et al. (1999) are cited for the data sources and the calculated heat capacity values are different from those calculated using the former workers' polynomials.

If only our DSC and the highest temperature PPMS data are used for fitting a C_p polynomial, one obtains in J/(mol·K)

$$C_p = 585.11(\pm 10) - 2263.40(\pm 354) \cdot T^{-0.5} - 1.90224(\pm 0.20) \cdot 10^7 \cdot T^{-2} + 2.422614(\pm 0.32) \cdot 10^9 \cdot T^{-3}. \quad (5)$$

This polynomial fits the experimental data with a slightly higher precision of $0.10 \pm 0.09\%$ compared to that given by Equation 4. Both polynomials give similar C_p values within 0.05% up to ~ 650 K. Above this temperature, extrapolated C_p values based on Equation 5 become increasingly larger, with a difference of $\sim 2\%$ at 2000 K (Fig. 11b). As a result, calculated relative enthalpies are larger above ~ 1100 K (Fig. 12) compared to the experimental values (Thiéblot et al. 1999). Thus, Equation 4 is recommended for extrapolation of C_p to high temperatures.

Heat capacity behavior of natural grossular

The raw PPMS and DSC C_p data collected on the four natural grossular samples are given in Appendix 2¹ (Supplementary information). The data are plotted in Figure 13 and Table 3 lists experimental details on the measurements. The agreement between PPMS and DSC heat capacities around ambient T is generally excellent. The DSC C_p values are very slightly larger from 0.1 to 0.7%. Sample coupling behavior for the single-crystal platelets is similar to that observed for the powder samples. At ambient temperature, sample coupling is $>99.1\%$ for all crystal platelets. We note, though, that measurements on single crystals with smaller masses (e.g., Gr-L/K weighing 15 mg) yield better sample coupling at higher temperatures, being nearly 100%, compared to measurements

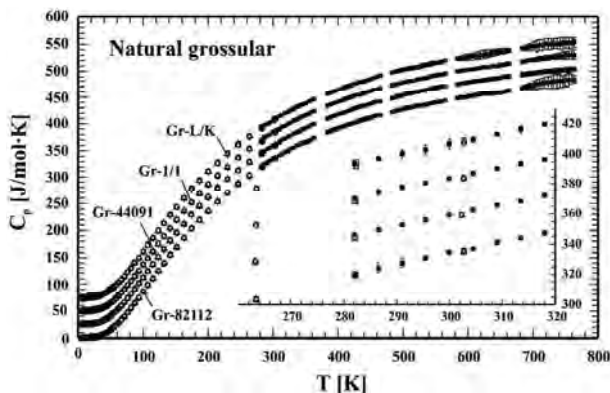


FIGURE 13. Measured low- and high-temperature heat-capacity values for the natural grossular samples Gr-82-112, Gr-44091, Gr-1/1, and Gr-L/K. Note that the C_p values for Gr-44091, Gr-1/1, and Gr-L/K are offset by +25, +50, and +75 J/(mol·K), respectively, to avoid overlap. Open symbols represent the PPMS measurements (the mean of the three PPMS C_p determinations at each temperature is shown), and the filled symbols the DSC data. The overlapping region between PPMS and DSC measurements is shown in the inset. Error bars represent 2σ and are for the PPMS measurements only shown in the inset.

on heavier single crystals. At low temperatures this behavior is reversed. The single-crystal platelets were made, therefore, after experimentation, to have a mass between 30 and 40 mg. This allows for optimal sample coupling behavior, with values better than 99% in most cases. This gives, we think, the most accurate heat-capacity determinations.

The experimental C_p uncertainties associated with the single-crystal measurements, $100(\sigma_{C_p}/C_p)$, are smaller compared to those on powders. For the former they amount to $\sim 0.2\%$ at $50 < T < 300$ K and are 1 to 2% at lower temperatures. In Figure 14a, we compare the low-temperature heat-capacity behavior of the various natural grossular samples (C_p^{nat}) to the final averaged values obtained from the three synthetic grossulars (C_p^{syn}). The percent difference $100(C_p^{\text{nat}} - C_p^{\text{syn}})/C_p^{\text{syn}}$ is plotted, where C_p^{syn} is calculated from Equation 3 and the parameters given in Supplementary Table 3¹. Above about 150 K, C_p values of natural and synthetic grossular are the same to better than 1%. Below this temperature down to ~ 25 K, all natural grossulars have smaller heat capacity values by up to $\sim 20\%$. The natural garnet showing the largest difference is the one that is closest to end-member grossular with $X_{\text{Gr}} = 0.97$ (i.e., Gr-82-112; see Table 4). Similar C_p behavior is shown by the natural grossulars investigated by Kolesnik et al. (1979) and Westrum et al. (1979) of composition $X_{\text{Gr}} = 0.95$ to 0.97 and $X_{\text{Gr}} = 0.91$, respectively (Table 4). In Figure 14b, the C_p values of both are compared to those of Haselton and Westrum (1980) obtained on synthetic grossular (Gr-Has). The grossular-rich sample studied by Kolesnik et al. (1979) generally has lower C_p values below 100 K, whereas the natural grossular of Westrum et al. (1979) shows less difference.

The relative uncertainties in C_p , $100(\sigma_{C_p}/C_p)$, from DSC measurements on the natural garnet platelets are between 0.2 to 0.5% at $300 < T < 600$ K and 0.4 to 2% at $T > 600$ K. The percent difference of the experimental values from the C_p

polynomial of Equation 4, obtained from synthetic grossular, is shown in Supplementary Figure 15¹. The heat-capacity values of the natural crystals are systematically slightly larger by 0.2 to 1%, with the exception of sample Gr-L/K, which has lower values at least to 600 K. These relative differences are, however, experimentally insignificant.

Entropy of natural grossular

The standard entropy determinations for a given sample show excellent reproducibility (Table 3). The values lie between 258.0 and 258.3 ± 1.0 J/(mol·K) for sample Gr-82-112, 260.9 and 261.2 ± 1.0 J/(mol·K) for Gr-44091 and 256.8 and 257.7 ± 1.1 J/(mol·K) for Gr-L/K. All three entropy determinations for Gr-44091 results from the fact that this sample contains more Fe and Mn than the other garnets (i.e., the sum of FeO + MnO amounts to ~ 2 wt%, whereas it is ~ 0.6 wt% in the other three natural grossulars, see Supplementary Table 2¹).

From these results, we calculate an adjusted standard entropy value for end-member grossular, S_{gr}° , for each natural garnet based on their compositions (Supplementary Table 3¹), assuming ideal thermodynamic mixing in garnet. For the calculations, we used the calorimetrically determined standard entropy values for spessartine $S_{\text{sp}}^{\circ} = 353.3$ J/(mol·K) (Dachs et al. 2009), pyrope $S_{\text{py}}^{\circ} = 266.27$ J/(mol·K) (Haselton and Westrum 1980), almandine $S_{\text{alm}}^{\circ} = 342.6$ J/(mol·K) (Anovitz et al. 1993), andradite $S_{\text{and}}^{\circ} = 316.4$ J/(mol·K) (Robie et al. 1987) and a S° value for katoite of $S_{\text{kat}}^{\circ} = 421.7$ J/(mol·K) (Geiger et al. 2012). For the other minor garnet components no S° values are available and they were treated as andradite.

We obtain for sample Gr-82-112

$$S_{\text{exp}}^{\circ} = 0.9714 S_{\text{gr}}^{\circ} + 0.0122 S_{\text{kat}}^{\circ} + 0.0012 S_{\text{sp}}^{\circ} + 0.0011 S_{\text{py}}^{\circ} + 0.0141 S_{\text{and}}^{\circ}; \quad (6a)$$

for sample Gr-44091

$$S_{\text{exp}}^{\circ} = 0.9404 S_{\text{gr}}^{\circ} + 0.0125 S_{\text{kat}}^{\circ} + 0.0138 S_{\text{sp}}^{\circ} + 0.0007 S_{\text{py}}^{\circ} + 0.0222 S_{\text{alm}}^{\circ} + 0.0104 S_{\text{and}}^{\circ}; \quad (6b)$$

for sample Gr-1/1

$$S_{\text{exp}}^{\circ} = 0.9438 S_{\text{gr}}^{\circ} + 0.0064 S_{\text{kat}}^{\circ} + 0.0035 S_{\text{sp}}^{\circ} + 0.011 S_{\text{py}}^{\circ} + 0.0353 S_{\text{and}}^{\circ}; \quad (6c)$$

and for sample Gr-L/K

$$S_{\text{exp}}^{\circ} = 0.9374 S_{\text{gr}}^{\circ} + 0.0077 S_{\text{kat}}^{\circ} + 0.0103 S_{\text{sp}}^{\circ} + 0.0155 S_{\text{py}}^{\circ} + 0.0293 S_{\text{and}}^{\circ}. \quad (6d)$$

The final adjusted values are $S^{\circ} = 255.1 \pm 1.2$ J/(mol·K) for Gr-82-112, $S^{\circ} = 255.2 \pm 1.2$ J/(mol·K) for Gr-44091, $S^{\circ} = 253.6 \pm 1.2$ J/(mol·K) for Gr-1/1, and $S^{\circ} = 253.0 \pm 1.2$ J/(mol·K) for Gr-L/K. It is important to note that the adjusted standard entropy value for each natural garnet is 5 to 7 J/(mol·K) smaller compared to the value of 260.23 ± 2.10 J/(mol·K) obtained from the synthetic grossular samples.

Supplementary Figure 16¹ shows the unadjusted S° values of

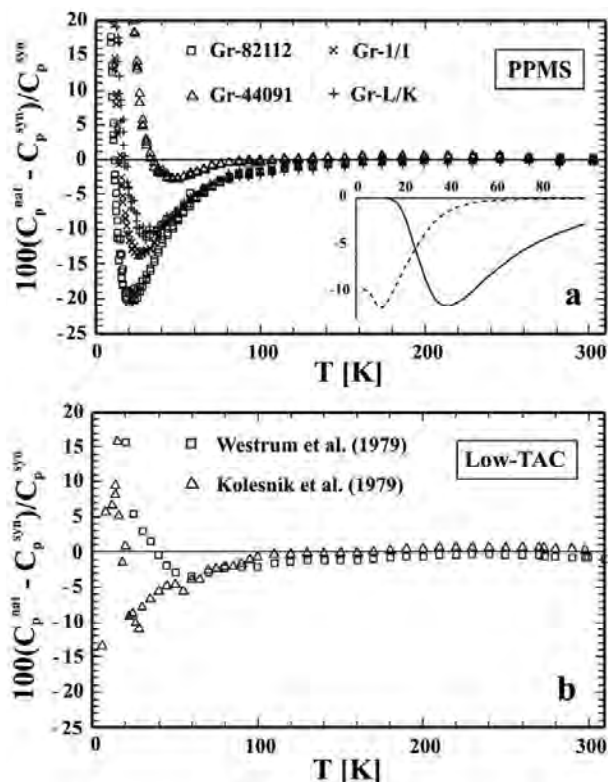


FIGURE 14. Percent difference plot of the low-temperature heat-capacity values of natural grossular (C_p^{nat}) vs. synthetic grossular (C_p^{syn}) for (a) the natural grossulars of this study: Gr-82-112 (squares), Gr-44091 (triangles), Gr-1/1 (X symbol), and Gr-L/K (crosses) and (b) for the natural grossulars studied using low-TAC by Westrum et al. (1979) (squares) and by Kolesnik et al. (1979) (triangles). The C_p^{syn} values in **a** have been calculated with the parameters given in Supplementary Table 4¹ and Equation 3 and in **b** based on the data of Haselton and Westrum (1980). The inset in **a** shows the percent difference calculated from modeling vibrational spectra assuming wavenumber differences between synthetic and natural garnets as discussed in the text.

the four natural grossulars plotted as a function of composition as given by the mole percent of their almandine plus andradite plus spessartine components. S° increases with increasing content of these components as expected. This plot also includes the unadjusted S° values from the studies of Westrum et al. (1979) and Kolesnik et al. (1979) on their natural grossular samples, i.e., $S^\circ = 259.5 \pm 0.8 \text{ J}/(\text{mol}\cdot\text{K})$ and $S^\circ = 259.7 \pm 1.3 \text{ J}/(\text{mol}\cdot\text{K})$, respectively. The former value has been calculated from the adjusted entropy given by Westrum et al. (1979, their Table 5) multiplied by the factor $453.132/450.454$, which is the quotient of the molar masses of their natural grossular over that of end-member grossular. Based on these data (Supplementary Fig. 16¹), one can make a linear fit and derive a standard entropy value for end-member grossular of $S^\circ = 257.6 \text{ J}/(\text{mol}\cdot\text{K})$. If one assumes further an average katoite content of 1% for all samples, this would give approximately $S^\circ = 255.9 \text{ J}/(\text{mol}\cdot\text{K})$. This value is close to that of $S^\circ = 255.2 \text{ J}/(\text{mol}\cdot\text{K})$, which is the mean value of the corrected entropy values obtained from Equations 6a–6d.

DISCUSSION

Composition and structural state of natural and synthetic grossular

The published and the present calorimetric results show that the C_p of natural grossular is less than that of synthetic grossular and thus the former gives slightly smaller S° values. The question is why are there differences in the heat capacity behavior between the two types of garnet. To address this question, it is mandatory to understand the chemical composition and structural state of the different grossular samples.

Natural garnets

The two natural grossulars from the Jeffrey mine studied herein, as well as the grossular sample from the Thetford mine (Westrum et al. 1979) and probably that of Kolesnik et al. (1979), crystallized in rhodinites. In the case of the Jeffrey mine locality the petrologic conditions, and the Thetford mine is probably similar, were investigated by Normand and William-Jones (2007). Crystallization occurred at relatively low temperatures at $<400^\circ\text{C}$ and in the presence of a fluid. In this case, grossular will have some structural OH (Fig. 6). For these garnets it is about 0.3% H_2O (Rossman and Aines 1991), corresponding to about 1.2–1.3 mol% when expressed as a katoite component (we stress again, however, that all the OH is substituting structurally in a manner that is not fully understood). The other two natural garnets from this study (Gr-L/K and Gr-1/1) have about 0.2 wt% H_2O (Rossman and Aines 1989) corresponding to $\sim 0.6\text{--}0.8$ mol% katoite. Green vanadium-rich grossulars from the Lualenyi mine in Kenya were metamorphosed under conditions of the upper amphibolite facies (Suwa et al. 1996) and the samples Gr-L/K and Gr-1/1 could be expected to have crystallized under similar conditions. Their slightly lower OH contents are consistent with their higher temperature of crystallization.

All natural grossulars contain other garnet components in solid solution. The sample Gr-82-112 studied here is one of the most grossular-rich garnets reported in the literature having about 97 mol% of the $\text{Ca}_3\text{Al}_2\text{Si}_3\text{O}_{12}$ component (Table 4). The other garnets have ~ 94 mol% $\text{Ca}_3\text{Al}_2\text{Si}_3\text{O}_{12}$ with other various minor garnet components in solid solution. The formula of the Thetford grossular, which was studied by Westrum et al. (1979), was recalculated using the formulism of Locock (2008) and it gives about 91% of a grossular component (Table 4). The grossular studied by Kolesnik et al. (1979), whose characterization was rudimentary, gives the composition $\text{Ca}_{3.02}\text{Fe}_{0.02}^{2+}\text{Mn}_{0.01}\text{Al}_{1.96}\text{Si}_{3.01}\text{O}_{12}$.

What about the structural state of natural grossulars? It has been shown that many grossulars crystallized at relatively low temperatures such as the samples Gr-82-112 and Gr-44098 are optically anisotropic (Allen and Buseck 1988; Rossman and Aines 1989; Akizuki 1989). Although considerable work has been done to try to explain the cause of the optical anisotropy, the effects are subtle and the origin is open to various interpretations (see Takéuchi et al. 1982; Allen and Buseck 1988; Rossman and Aines 1989; Akizuki 1989). It does appear, though, that partial ordering of Al-Fe³⁺ and Ca-Fe²⁺ can occur on the octahedral and dodecahedral sites, respectively, in space groups lower than cubic symmetry (Takéuchi et al. 1982; Allen and Buseck 1988). The

issue of optical behavior was not addressed in the calorimetric studies of Westrum et al. (1979) and Kolesnik et al. (1979), but we view it as likely that their grossular samples were also anisotropic. The grossular samples Gr-L/K and Gr-1/1 from this work are, in contrast, isotropic. This is consistent with their interpreted higher temperature crystallization conditions and they are considered to be cubic of space group symmetry $Ia\bar{3}d$.

Synthetic grossular

The synthetic grossular samples studied here were crystallized, in contrast to the naturals, at elevated pressures at temperatures from 1000 to 1250 °C in a fluid-free environment (Table 1). The microprobe results for two of the samples (Gr-92 and Gr-Has) are not straightforward to interpret in a precise manner. If they are correct, then these samples show small deviations from end-member grossular stoichiometry, above an analytical uncertainty that should be about 1% for the different cation numbers in the formula unit. We have noted in several investigations over the years difficulties in obtaining exact stoichiometric formulas on various synthetic aluminosilicate garnets using the electron microprobe (e.g. Geiger et al. 1987; Dachs et al. 2009). It is not clear whether the results are reflecting analytical artifacts (minor problems in data correction programs, fine grain sizes of the polycrystalline samples, etc.) or whether they are showing slight but real compositional deviations. Work is needed in this area and is presently being undertaken (Fournelle and Geiger 2010). The third synthetic sample, Gr-Kiel, shows good grossular stoichiometry.

All three samples contain a very minor amount of wollastonite. It is not clear how or at what stage during synthesis that this phase arose. It is notable that it is found in all samples regardless of the lab it was synthesized in and under what conditions. The presence of wollastonite would seem to require the presence of other phases such as anorthite, gehlinit, or corundum, but neither they nor any other aluminous phase could be identified in the synthetic samples.

X-ray crystal structure refinements of synthetic grossular indicate garnet stoichiometry and complete long-range ordering (Geiger and Armbruster 1997; Rodehorst et al. 2002), but it may still be possible to have slight Al-Si disorder. NMR spectroscopy is an excellent experimental method to address the question of order-disorder in garnet (Geiger et al. 1992; Bosenick et al. 1995; Kelsey et al. 2008). The ^{29}Si NMR spectra of synthetic grossulars Gr-35 and Gr-Has, the former of which was synthesized under similar conditions as Gr-Has, Gr-92, and Gr-Kiel, shows a single, strong, and narrow resonance at -83.9 ppm (Fig. 4) that can be assigned to Si in tetrahedral coordination (Bosenick et al. 1995; Geiger 2004). The spectrum does not appear to show any additional resonance between about -180 and -220 , which could be assigned to octahedrally coordinated Si (Stebbins 1995). An analogous conclusion is made from the ^{27}Al NMR spectrum of synthetic grossular Gr-35, which does not show any overt evidence for AlO_4 groups (see Stebbins 1995). Based on these NMR results, we find no evidence for Al-Si disorder in the synthetic grossulars. The presence of Al-Si octahedral-tetrahedral disorder in end-member grossular (or any other common aluminosilicate garnet) has not been noted before to the best of our knowledge, but further work is needed to fully verify this.

As to the question of impurities, wollastonite shows Si resonances at -87.6 and -91.7 ppm (Stebbins 1995), but there is no indication for these resonances in the ^{29}Si NMR spectrum of Gr-Has (Fig. 4b).

C_p behavior of natural vs. synthetic grossular: What is S° for stoichiometric end-member grossular?

The major difference between synthetic and natural grossulars in terms of heat capacity is that the latter have lower C_p values by up to $\sim 20\%$ between 20 and 100 K (Fig. 14a). To try to understand this observation, we calculated C_p behavior by using the simplified vibrational density of states model for grossular of Chopelas (2006). We lowered the lower wavenumber cut-off for two of the six optical continua by 12 cm^{-1} , whereby these lower limits are given by 159 cm^{-1} for the optical continuum 1 and 178 cm^{-1} for the optical continuum 2. The final result of this exercise is shown as the inset in Figure 14a. The calculation indicates that wavenumber variations for low-energy optical phonons on the order of 10% could produce the observed differences in the heat-capacity behavior. However, an inspection of published IR spectra of synthetic and natural grossulars shows no significant differences between the energies of their IR modes at low wavenumbers (Geiger 1998; Bosenick et al. 1995; Boffa Ballaran et al. 1999; McAloon and Hofmeister 1993). If, on the other hand, the acoustic modes are shifted by 3 cm^{-1} upward in energy for natural grossular compared to synthetic grossular, similar C_p behavior is observed (inset in Fig. 14a). Its minimum lies at somewhat lower temperatures compared to the observed behavior. However, experimental sound velocities are not available for both synthetic and natural grossular to fully test this hypothesis.

The data of this work confirm the results of earlier low-temperature calorimetric studies (Westrum et al. 1979; Kolesnik et al. 1979; Haselton and Westrum 1980) that show small differences in S° between natural and synthetic grossular samples. To obtain S° for end-member grossular, Westrum et al. (1979) made corrections for the various solid-solution components occurring in their Thetford grossular sample. They assigned entropy contributions from almandine (3.8 mol%), spessartine (1.4 mol%), Mg-melanite (1.4 mol%), pyrope (0.4 mol%), and hydrogrossular (2.4 mol%) and considered that they mix ideally in grossular. To obtain a S° value for hydrogrossular an approximation was adopted using brucite, $\text{Mg}(\text{OH})_2$. We reanalyzed their experimental heat capacity data using the crystal chemical formula in Table 4. Using published S° values for the various minor end-member garnet components, and also using an S° value for katoite of $421.7\text{ J}/(\text{mol}\cdot\text{K})$ (Geiger et al. 2012), as well as taking the S° values for the very small schorlomite-Al and morimotoite components as those of andradite, we obtain an adjusted value for end-member grossular of $S^\circ = 254.4\text{ J}/(\text{mol}\cdot\text{K})$ in agreement with their value of $254.72 \pm 0.84\text{ J}/(\text{mol}\cdot\text{K})$. The lower S° for their natural grossular, and for our samples as well, compared to synthetic grossular cannot be explained based on this simple type of analysis.

However, it is assumed that the vibrational entropy of mixing behavior in garnet is ideal. This may not be quantitatively correct. Consider, for example, the entropy of mixing of binary pyrope-grossular garnets (Dachs and Geiger 2006). Here, depending on the type of model used to describe the entropy

of mixing behavior at 298 K, a positive excess contribution of roughly 2 J/(mol·K), compared to a mechanical mixture, can arise for garnet compositions at about 0.1 mole fraction removed from an end-member. Of course, in this case, this involves Ca-Mg mixing at the X-site. In the case of natural grossulars the solid solution is more complex, because atomic mixing occurs at both the X- and Y-sites and also various OH substitutional mechanisms may operate. Because of lack of data describing the entropy of mixing behavior for Y-site cations, a more quantitative analysis cannot be made. We do note that the difference in the molar volume between grossular and katoite is large and therefore solid solutions between the two could be associated with large nonideal mixing behavior (Geiger 1999; Bosenick et al. 2001). We conclude that the entropy of mixing behavior in these garnets could be nonideal and the assumption of ideal mixing to adjust S° values for natural grossulars may not be quantitatively correct.

A possible complication regarding the experimental C_p data of synthetic grossular involves the presence of minor amounts of wollastonite in the samples (Supplementary Figs. 2¹ and 3¹). The question arises if it could affect the calorimetrically determined S° value in a significant manner. To test this possibility, we assumed that synthetic grossular contains wollastonite and corundum in the molar ratio 3:1, as based on the reaction grossular = 3wollastonite + corundum. We then calculated the C_p contribution of these two phases to the measured C_p values

TABLE 5. Standard thermodynamic properties for grossular from various studies

$\Delta_f H^\circ$ (kJ/mol)	S° [J/(mol·K)]	Reference
-6632.86	255.15	Berman (1988)
-6640.0 ± 3.2	260.1 ± 0.5	Robie and Hemingway (1995)
-6632.18 ± 0.78	257.47 ± 0.24	Gottschalk (1997)
-6644.07 ± 1.60	255.00	Holland and Powell (1998)
-6639.56 ± 1.31	259.96 ± 0.48	Chatterjee et al. (1998)
-6642.95 ± 1.46	255.00	Holland and Powell (2011)
-6627.00	258.8	Calculated in this study

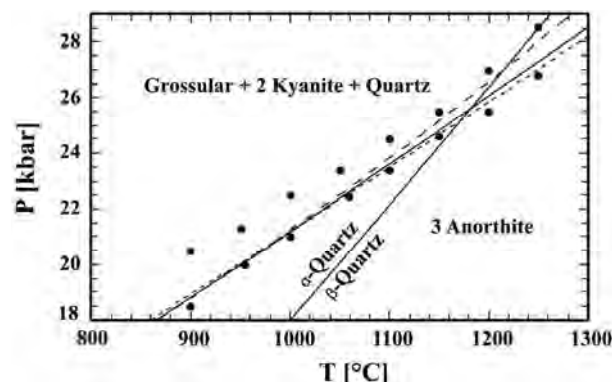


FIGURE 18. Experimental brackets on the GASP reaction (grossular + 2 kyanite + quartz = 3 anorthite) depicted by solid circles (Koziol and Newton 1988). The calculated GASP reaction is shown by a short-dashed line. The long-dashed curve shows the same calculation but includes a temperature-dependent S^{circ} term for Al-Si disorder in anorthite according to Myers et al. (1998) and is calculated with grossular standard state properties of $S^\circ = 258.8$ J/(mol·K) and $\Delta_f H^\circ = -6629$ kJ/mol. The reaction after Berman (1988) is shown by the solid line.

as a function of their amounts. For these calculations we used the C_p data of grossular from Haselton and Westrum (1980). Thus, for example, synthetic grossular containing hypothetically 1 vol% wollastonite and 0.33 vol% corundum S° would be lowered from the value of grossular alone by 0.36 J/(mol·K). The complete results of this exercise are shown in Supplementary Figure 17¹ that gives S° for grossular as a function of the volume percent wollastonite + corundum.

To lower the S° value of synthetic grossular by about 5 to 7 J/(mol·K) to bring it in line with a value of about 253 to 255 J/(mol·K) as given by the natural grossulars, the synthetic material would have to contain about 12 vol% wollastonite. Clearly, such a large amount is not in accordance with the amount obtained from the XRD patterns and optical examination giving ~1 to 2 vol%. We conclude that $S^\circ \approx 260$ J/(mol·K) represents the best value for stoichiometric end-member grossular.

Phase equilibrium in the CASH system and thermodynamic properties of grossular

Experimentally determined phase equilibrium relations in the CAS(H) system should be dependent on the grossular garnet used for study, i.e., natural garnet vs. synthetic grossular. Small differences in the P - T positions of various univariant reactions involving grossular could be expected. We compared experimental brackets on the univariant equilibrium reactions



and



as investigated in various studies using different garnet starting materials (i.e., Newton 1965, 1966; Boettcher 1970; Chatterjee et al. 1984). There are, however, no observable differences between the various experimental results for Equations 7 and 8.

There is a range of S° values present in the literature for grossular. The S° value presented in Chatterjee et al. (1998) of 259.962 ± 0.483 J/(mol·K) is closest to our value for synthetic grossular. The Holland and Powell (1998, 2011) and Berman (1988) databases list values that are closer to S° obtained on natural samples, namely 255.10 and 255.00 J/(mol·K), respectively. Gottschalk's (1997) S° value for grossular of 257.469 ± 0.243 J/(mol·K) falls between the highest and lowest measured values (Table 5). Berman (1988) argued that a S° value of about 260 J/(mol·K) was not consistent with his mathematical programming (MAP) analysis of various phase equilibria.

We address this issue using MAP (Berman et al. 1986; Grevel et al. 2001; Grevel 2004) and by analyzing the reaction



Reaction 9 is chosen because it is one of the "simpler" reactions in the CASH system and because it has been carefully reversed in P - T space (i.e., Koziol and Newton 1988). Input thermodynamic data for kyanite, quartz, and anorthite were taken from Berman (1988). The thermal expansion of grossular is taken as

$$V/V^{\circ} = 1 + 2.2917 \cdot 10^{-5} (T - 298.15) + 0.54603 \cdot 10^{-8} (T - 298.15)^2, \quad (10)$$

whereby the constants were obtained by fitting the thermal expansion data for grossular of Isaak et al. (1992). V° of grossular was taken as 125.3 cm³/mol and its pressure dependence was taken from Berman (1988). The C_p behavior and the starting value of S° for grossular are from this work. Applying the MAP analysis to Equation 9, we obtain $\Delta_r H^{\circ} = -6627.0$ kJ/mol and $S^{\circ} = 258.8$ J/(mol·K) for grossular (Table 5). As can be seen from Figure 18, the reversal brackets on Equation 9 (which were not available at the time that Berman derived his database) can be fit with both Berman's (1988) data and also using the S° value for synthetic grossular.

We note that for completeness that the MAP procedure should be undertaken using all available equilibria involving grossular and thermodynamic data for other phases of interest, but this is far beyond the scope of this study. Such a treatment should also include any configurational entropy contributions relating to Al-Si disorder in anorthite (e.g., Myers et al. 1998) that may become important at high temperatures (Fig. 18).

High-temperature extrapolation of the DSC results

We used the relative enthalpy data of Thiéblot et al. (1999) to constrain our C_p polynomial (Eq. 4) at high temperatures. One can, alternatively, following Holland (1981), extrapolate the heat capacity behavior for grossular based on the approximation $C_p^{\text{grossular}} = 3C_p^{\text{wollastonite}} + C_p^{\text{corundum}}$. However, this procedure gives rather unsatisfactory results as shown in Figure 11. This approximation leads, using the Holland and Powell (1998 2011) data set for the necessary C_p values, to relative enthalpies that are higher by 0.4 to more than 1% than the experimental values. At 2000 K, the heat capacity based on this approximation is too high by nearly 4% (Fig. 11). With the Berman (1988) data set it would be too high by 2.3% at this temperature.

ACKNOWLEDGMENTS

We thank N.-S. Rahmoun and G. Tippet for help in making the IR and X-ray powder diffraction measurements, as well as A. Fehler for making the polished crystal platelets. The Jeffrey mine samples were kindly donated by M. Picard from the Canadian Museum of Nature, the grossular samples Gr-1/1 and Gr-L/K by K. Langer and T. Haselton generously contributed his synthetic grossular. Xianyu Xue provided helpful discussion on the NMR results. This work was financed by grants P21370-N21 and P23056-N21 from the Austrian Science Fund (FWF).

REFERENCES CITED

- Allen, F.M. and Buseck, P.R. (1988) XRD, FTIR, and TEM studies of optically anisotropic grossular garnets. *American Mineralogist*, 73, 568–584.
- Akizuki, M. (1989) Growth structure and crystal symmetry of grossular garnets from the Jeffrey mine, Asbestos, Quebec, Canada. *American Mineralogist*, 74, 859–864.
- Anovitz, L.M., Essene, E.J., Metz, G.W., Bohlen, S.R., Westrum, E.F. Jr., and Hemingway, B.S. (1993) Heat capacity and phase equilibria of almandine, Fe₂Al₂Si₂O₁₂. *Geochimica et Cosmochimica Acta*, 57, 4191–4204.
- Benisek, A. and Dachs, E. (2008) The uncertainty in determining the third law entropy by the heat-pulse calorimetric technique. *Cryogenics*, 48, 527–529.
- Berman, R.G. (1988) Internally-consistent thermodynamic data for minerals in the system Na₂O-K₂O-CaO-MgO-FeO-Fe₂O₃-Al₂O₃-SiO₂-TiO₂-H₂O-CO₂. *Journal of Petrology*, 29, 445–522.
- Berman, R.G. and Brown, T.H. (1985) Heat capacity of minerals in the system Na₂O-K₂O-CaO-MgO-FeO-Fe₂O₃-Al₂O₃-SiO₂-TiO₂-H₂O-CO₂: representation, estimation, and high temperature extrapolation. *Contributions to Mineralogy and Petrology*, 89, 168–183.
- Berman, R.G., Engi, M., Greenwood, H.J., and Brown, T.H. (1986) Derivation of

- internally-consistent thermodynamic data by the technique of mathematical programming: a review with application to the system MgO-SiO₂-H₂O. *Journal of Petrology*, 27, 1331–1364.
- Boettcher, A.L. (1970) The system CaO-Al₂O₃-SiO₂-H₂O at high pressures and temperatures. *Journal of Petrology*, 11, 337–379.
- Boffa Ballaran, T., Carpenter, M.A., Geiger, C.A., and Koziol, A. (1999) Local structural heterogeneity in garnet solid solutions. *Physics and Chemistry of Minerals*, 26, 554–569.
- Boerio-Goates, J., Stevens, R., Hom, B.K., Woodfield, B.F., Piccione, P.M., Davis, M.E., and Navrotsky, A. (2002) Heat capacities, third-law entropies and thermodynamic functions of SiO₂ molecular sieves from T = 0 K to 400 K. *Journal of Chemical Thermodynamics*, 34, 205–227.
- Bosenick, A., Geiger, C.A., Schaller, T., and Sebald, A. (1995) A ²⁹Si MAS NMR and IR spectroscopic investigation of synthetic pyrope-grossular garnet solid solutions. *American Mineralogist*, 80, 691–704.
- Bosenick, A., Geiger, C.A., and Cemič, L. (1996) Heat capacity measurements of synthetic pyrope-grossular garnets between 320 and 1000 K by differential scanning calorimetry. *Geochimica et Cosmochimica Acta*, 60, 3215–3227.
- Bosenick, A., Dove, M.T., Heine, V., and Geiger, C.A. (2001) Scaling of thermodynamic mixing properties in solid solution minerals. *Physics and Chemistry of Minerals*, 28, 177–187.
- Chatterjee, N.D., Johannes, W., and Leistner, H. (1984) The system CaO-Al₂O₃-SiO₂-H₂O: new phase equilibria data, some calculated phase relations, and their petrological applications. *Contributions to Mineralogy and Petrology*, 88, 1–13.
- Chatterjee, N.D., Krüger, R., Haller, G., and Olbricht, W. (1998) The Bayesian approach to an internally consistent thermodynamic database: theory, database, and generation of phase diagrams. *Contributions to Mineralogy and Petrology*, 133, 149–168.
- Chopelas, A. (2006) Modeling the thermodynamic parameters of six endmember garnets at ambient and high pressures from vibrational data. *Physics and Chemistry of Minerals*, 33, 363–376.
- Dachs, E. and Benisek, A. (2011) A sample-saving method for heat capacity measurements on powders using relaxation calorimetry. *Cryogenics*, 51, 460–464.
- Dachs, E. and Bertoldi, C. (2005) Precision and accuracy of the heat-pulse calorimetric technique: Low-temperature heat capacities of milligram-sized synthetic mineral samples. *European Journal of Mineralogy*, 17, 251–261.
- Dachs, E. and Geiger, C.A. (2006) Heat capacities and entropies of mixing of pyrope-grossular (Mg₃Al₂Si₂O₁₂-Ca₃Al₂Si₂O₁₂) garnet solid solutions: a low temperature calorimetric and a thermodynamic investigation. *American Mineralogist*, 91, 894–906.
- Dachs, E., Geiger, C.A., Withers, A.C., and Essene, E.J. (2009) A calorimetric investigation of spessartine: vibrational and magnetic heat capacity. *Geochimica et Cosmochimica Acta*, 73, 3393–3409.
- Dachs, E., Benisek, A., and Geiger, C.A. (2010) Relaxation calorimetry applied to mineralogical samples: Results from the Salzburg calorimetry laboratory. IUPAC International Conference on Chemical Thermodynamics 2010, Tsukuba Science City, Ibaraki, Japan; abstract CC-2202-1110S.
- Dachs, E., Geiger, C.A., and Benisek, A. (2012) Almandine: Lattice and non-lattice heat capacity behavior and standard thermodynamic properties. *American Mineralogist*, in press.
- Ditmars, D.A., Ishihara, S., Chang, S.S., Bernstein, G., and West, E.D. (1982) Measurements of the relative enthalpy of pure α-Al₂O₃ (NBS heat capacity and enthalpy standard reference material no. 720) from 10 to 1,950 K. *Journal Research of the National Bureau of Standards*, 87, 5–9.
- Fournelle, J. and Geiger, C.A. (2010) An electron microprobe study of synthetic aluminosilicate garnets. *American Geophysical Union, Fall Meeting 2010*, abstract V51C-2208.
- Geiger, C.A. (1998) A powder infrared spectroscopic investigation of garnet binaries in the system Mg₃Al₂Si₂O₁₂-Fe₃Al₂Si₂O₁₂-Mn₃Al₂Si₂O₁₂-Ca₃Al₂Si₂O₁₂. *European Journal of Mineralogy*, 3, 407–422.
- (1999) Thermodynamics of (Fe²⁺, Mn²⁺, Mg, Ca)₃Al₂Si₂O₁₂ garnet: a review and analysis. *Mineralogy and Petrology*, 66, 271–299.
- (2004) Spectroscopic investigations relating to the structural, crystal-chemical and lattice-dynamic properties of (Fe²⁺, Mn²⁺, Mg, Ca)₃Al₂Si₂O₁₂ garnet: A review and analysis. In E. Libowitzky and A. Beran, Eds., *Spectroscopic Methods in Mineralogy*, 6, p. 589–645. *European Mineralogical Union (EMU) Notes in Mineralogy*, Eötvös University Press, Budapest.
- Geiger, C.A. and Armbruster, T. (1997) Mn₃Al₂Si₂O₁₂ spessartine and Ca₃Al₂Si₂O₁₂ grossular garnet: dynamical structural and thermodynamic properties. *American Mineralogist*, 82, 740–747.
- Geiger, C.A., Newton, R.C., and Kleppa, O.J. (1987) Enthalpy of mixing of synthetic almandine-grossular and almandine-pyrope garnets from high-temperature solution calorimetry. *Geochimica et Cosmochimica Acta*, 51, 1755–1763.
- Geiger, C.A., Merwin, L., and Sebald, A. (1992) Structural investigation of pyrope garnet using temperature-dependent FTIR and ²⁹Si and ²⁷Al MAS NMR spectroscopy. *American Mineralogist*, 77, 713–717.
- Geiger, C.A., Stahl, A., and Rossmann, G.R. (2000) Single-crystal IR- and UV/VIS-spectroscopic measurements on transition-metal-bearing pyrope: The

- incorporation of hydroxal in garnet. *European Journal of Mineralogy*, 12, 259–271.
- Geiger, C.A., Dachs, E., and Benisek, A. (2012) Thermodynamic behavior and properties of katoite (hydrogrossular): A calorimetric study. *American Mineralogist*, 97, 1252–1255.
- Gottschalk, M. (1997) Internally consistent thermodynamic data for rock-forming minerals in the system $\text{SiO}_2\text{-TiO}_2\text{-Al}_2\text{O}_3\text{-Fe}_2\text{O}_3\text{-CaO-MgO-FeO-K}_2\text{O-Na}_2\text{O-H}_2\text{O-CO}_2$. *European Journal of Mineralogy*, 9, 175–223.
- Grevel, K.-D. (2004) Intern konsistente thermodynamische Daten für ausgewählte Hochdruckphasen im System $\text{CaO-MgO-Al}_2\text{O}_3\text{-SiO}_2\text{-H}_2\text{O}$. Habilitation thesis (partly in German), Ruhr University Bochum, Germany, VII + 113p.
- Grevel, K.-D., Schoenitz, M., Skrok, V., Navrotsky, A., and Schreyer, W. (2001) Thermodynamic data of lawsonite and zoisite in the system $\text{CaO-Al}_2\text{O}_3\text{-SiO}_2\text{-H}_2\text{O}$ based on experimental phase equilibria and calorimetric work. *Contributions to Mineralogy and Petrology*, 142, 298–308.
- Haselton, H.T. (1979) Calorimetry of synthetic pyrope-grossular garnets and calculated stability relations. Ph.D. thesis, University of Chicago.
- Haselton, H.T. Jr. and Westrum, E.F. Jr. (1980) Low-temperature heat capacities of synthetic pyrope, grossular, and pyrope₆₀grossular₄₀. *Geochimica et Cosmochimica Acta*, 44, 701–709.
- Hofmeister, A.M. and Chopelas, A. (1991) Thermodynamic properties of pyrope and grossular from vibrational spectroscopy. *American Mineralogist*, 76, 880–891.
- Holland, T.J.B. (1981) Thermodynamic analysis of simple mineral systems. In R.C. Newton, A. Navrotsky, and B.J. Wood, Eds., *Thermodynamics of minerals and melts*, pp. 19–34. Springer Verlag, New York.
- Holland, T.J.B. and Powell, R. (1998) An internally consistent thermodynamic data set for phases of petrological interest. *Journal of Metamorphic Geology*, 16, 309–343.
- (2011) An improved and extended internally consistent thermodynamic dataset for phases of petrological interest, involving a new equation of state for solids. *Journal of Metamorphic Geology*, 29, 333–383.
- Hwang, J.S., Lin, K.J., and Tien, C. (1997) Measurement of heat capacity by fitting the whole temperature response of a heat-pulse calorimeter. *Review of Scientific Instruments*, 68(1), 94–101.
- Isaak, D.G., Anderson, O.L., and Oda, H. (1992) High-temperature thermal expansion and elasticity of calcium-rich garnets. *Physics and Chemistry of Minerals*, 19, 106–120.
- Kelsey, K.E., Stebbins, J.F., Du L.-S., Mosenfelder, J.L., Asimow, P.D., and Geiger, C.A. (2008) Cation order/disorder behavior and crystal chemistry of pyrope-grossular garnets: An ^{17}O QMAS and ^{27}Al MAS NMR spectroscopic study. *American Mineralogist*, 93, 134–143.
- Kolesnik, Yu.N., Nogteva, V.V., Arkhipenko, D.K., Orekhov, B.A., and Ye, I. (1979) Thermodynamics of pyrope-grossular solid solutions and the specific heat of grossular at 13–300 K. *Geochemistry International*, 16(3), 57–64.
- Kolesov, B.A. and Geiger, C.A. (2005) The vibrational spectrum of synthetic hydrogrossular (Katoite) $\text{Ca}_3\text{Al}_2(\text{O}_2\text{H}_4)_2$: A low temperature IR and Raman spectroscopic study. *American Mineralogist*, 90, 1335–1341.
- Koziol, A.M. and Newton, R.C. (1988) Redetermination of the anorthite breakdown reaction and improvement of the plagioclase-garnet- Al_2SiO_5 -quartz barometer. *American Mineralogist*, 73, 216–223.
- Krupka, K.M., Robie, R.A., and Hemingway, B.S. (1979) High-temperature heat capacities of corundum, periclase, anorthite, $\text{CaAl}_2\text{Si}_2\text{O}_8$ glass, muscovite, pyrophyllite, KAlSi_3O_8 , grossular and $\text{NaAlSi}_3\text{O}_8$ glass. *American Mineralogist*, 64, 86–101.
- Lashley, J.C., Hundley, M.F., Migliori, A., Sarrao, J.L., Pagliuso, P.G., Darling, T.W., Jaime, M., Cooley, J.C., Hults, W.L., Morales, L., and others. (2003) Critical examination of heat capacity measurements made on a Quantum Design physical property measurement system. *Cryogenics*, 43, 369–378.
- Locock, A.J. (2008) An Excel spreadsheet to recast analyses of garnet into end-member components, and a synopsis of the crystal chemistry of natural silicate garnets. *Computers and Geoscience*, 34, 1769–1780.
- McAloon, B.P. and Hofmeister, A.M. (1993) Single-crystal absorption and reflection infrared spectroscopy of birefringent grossular-andradite garnets. *American Mineralogist*, 78, 957–967.
- Mraw, S.C. (1988) Differential scanning calorimetry. In C.Y. Ho, Ed., *Data Series on Material Properties*, 1–2, p. 395–437. Hemisphere, New York.
- Myers, E.R., Heine, V., and Dove, M. (1998) Thermodynamics of Al/Al avoidance in the ordering of Al/Si tetrahedral framework structures. *Physics and Chemistry of Minerals*, 25, 457–464.
- Newton, R.C. (1965) The thermal stability of zoisite. *Journal of Geology*, 73, 431–441.
- (1966) Some calc-silicate equilibrium relations. *American Journal of Science*, 264, 204–222.
- Normand, C. and William-Jones, A.E. (2007) Physicochemical conditions and timing of rodingite formation: evidence from rodingite-hosted fluid inclusions in the JM Asbestos mine, Asbestos, Québec. *Geochemical Transactions*, 8:11, 1–19.
- Perkins, D. III, Essene, E.J., Westrum, E.F. Jr., and Wall, V.J. (1977) Application of new thermodynamic data to grossular phase relations. *Contributions to Mineralogy and Petrology*, 64, 137–147.
- Pilati, T., Demartin, F., and Gramaccioli, C.M. (1996) Atomic displacement parameters for garnets: A lattice-dynamical evaluation. *Acta Crystallographica*, B52, 239–250.
- Robie, R.A. and Hemingway, B.S. (1972) Calorimeters for heat of solution and low-temperature heat capacity measurements. U.S. Geological Survey Professional Paper, 755, 1–32.
- (1995) Thermodynamic Properties of Minerals and Related Substances at 298.15 K and 1 Bar (10^5 Pascals) Pressure and at Higher Temperatures. U.S. Geological Survey Bulletin, 2131, 461 p.
- Robie, R.A., Zhao, B., Hemingway, B.S., and Barton, M.S. (1987) Heat capacities and thermodynamic properties of andradite garnet, $\text{Ca}_3\text{Fe}_2\text{Si}_3\text{O}_{12}$, between 10 and 1000K and revised values for $\Delta_f G_m^\circ$ (298.15 K) of hedenbergite and wolastonite. grossular garnets between 320 and 1000 K by differential scanning calorimetry. *Geochimica et Cosmochimica Acta*, 51, 2219–2224.
- Rodehorst, U., Geiger, C.A., and Armbruster, T. (2002) The crystal structure of synthetic grossular and spessartine between 100 and 600 K and the crystal chemistry of grossular-spessartine solid solutions. *American Mineralogist*, 87, 542–549.
- Rossman, G.R. and Aines, R.D. (1989) Spectroscopy of a birefringent grossular from Asbestos, Quebec, Canada. *American Mineralogist*, 71, 779–780.
- (1991) The hydrous components in garnets: Grossular-hydrogrossular. *American Mineralogist*, 76, 1153–1164.
- Stebbins J.F. (1995) Nuclear magnetic resonance spectroscopy of silicates and oxides in geochemistry and geophysics. In T.J. Ahrens, Ed., *Mineral Physics and Crystallography: A Handbook of Physical Constants*, pp. 303–332. American Geophysical Union, Washington, D.C.
- Suwa, K., Suzuki, K., and Agata, T. (1996) Vanadium grossular from the Mozambique metamorphic rocks, south Kenya. *Journal of Southeast Asian Earth Sciences*, 14, 299–308.
- Takéuchi, Y., Haga, N., Umizu, S., and Sato, G. (1982) The derivative structure of silicate garnets in grandite. *Zeitschrift für Kristallographie*, 158, 53–99.
- Thiéblot, L., Téqui, C., and Richet, P. (1999) High-temperature heat capacity of grossular ($\text{Ca}_3\text{Al}_2\text{Si}_3\text{O}_{12}$), enstatite (MgSiO_3), and titanite (CaTiSiO_5). *American Mineralogist*, 84, 848–855.
- Westrum, E.F. Jr., Essene, E.J., and Perkins, D. III (1979) Thermophysical properties of the garnet, grossular: $\text{Ca}_3\text{Al}_2\text{Si}_3\text{O}_{12}$. *Journal of Chemical Thermodynamics*, 11, 57–66.

MANUSCRIPT RECEIVED NOVEMBER 14, 2011

MANUSCRIPT ACCEPTED APRIL 25, 2012

MANUSCRIPT HANDLED BY BJORN MYSEN